Be electrical

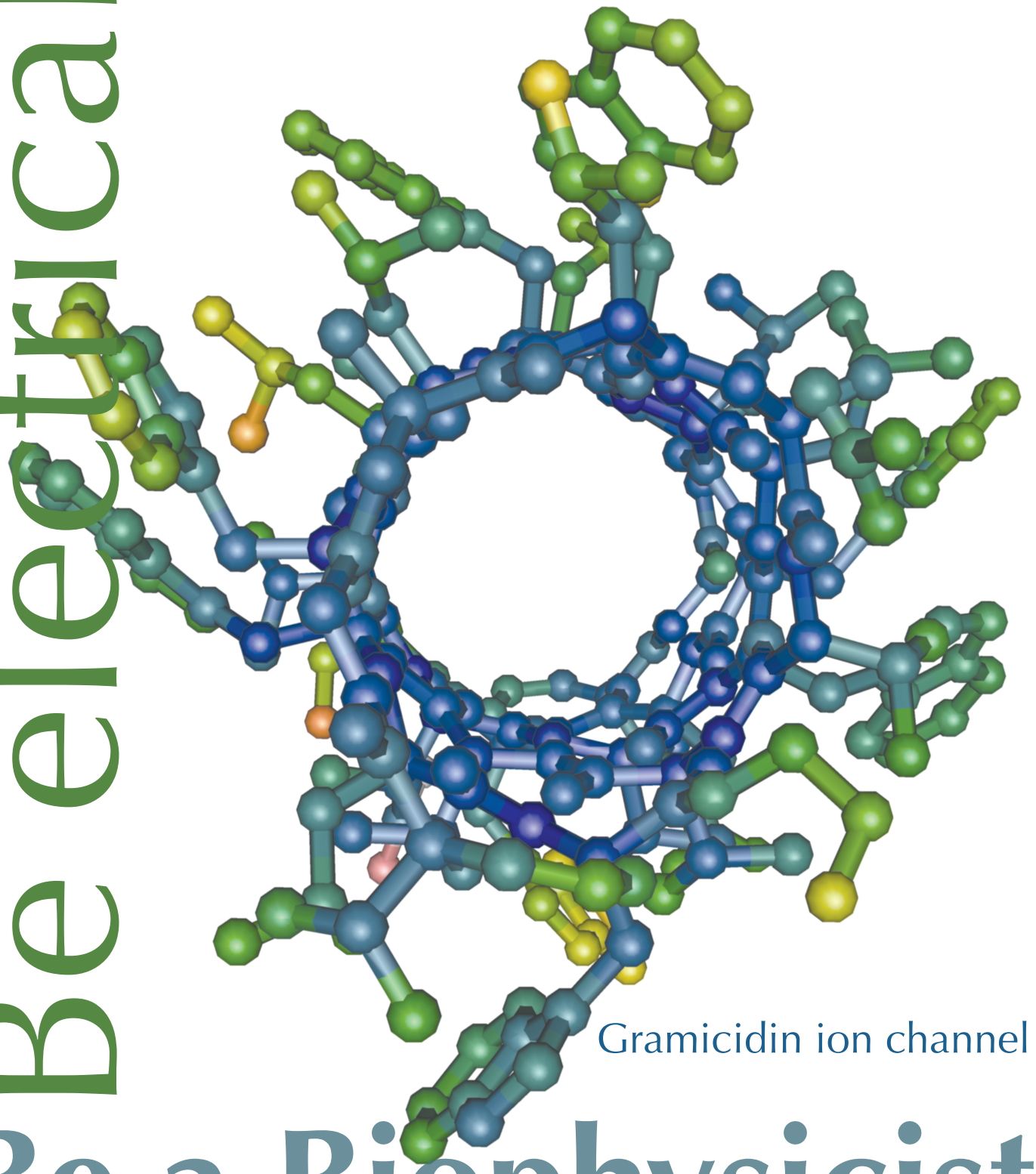

Gramicidin ion channel

Be a Biophysicist

Current Topics in Biophysics
(SC/BPHS 2090 2.0)

Biophysical Currents

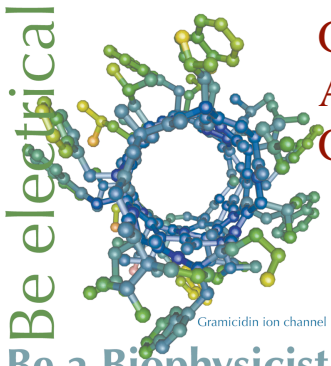

Gramicidin: A Model Ion Channel

Current Topics in Biophysics
(SC/BPHS 2090 2.0)

Biophysical Currents

Ion permeation through Gramicidin A

by multiscale

(vimeo: http://vimeo.com/3173968)

A potassium ion (green) crosses a membrane by passing through the Gramicidin A pore.

This is a steered molecular modeling of all 29000 atoms of the system for approximately 3 microseconds. Water and membrane molecules are hidden for clarity.

The underlying simulations were performed thanks to the PS3 time generously donated by the contributors to the gpugrid.net project.

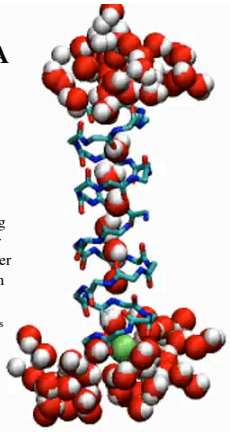

Ion permeation through Gramicidin A

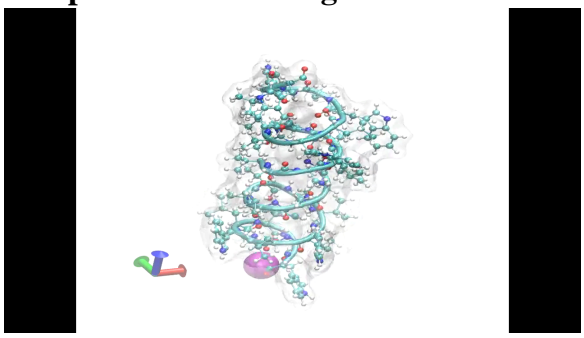

by multiscalelab (vimeo: http://vimeo.com/9649709) A potassium ion (purple) crosses a membrane by passing through the Gramicidin A pore.

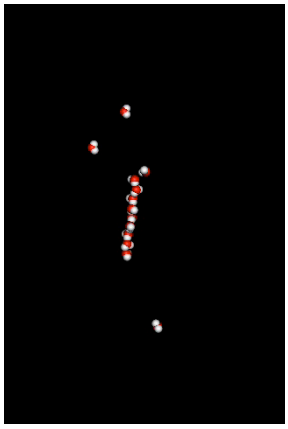

1.2 NSEC OF WATER MOVEMENT IN A GRAMICIDIN CHANNEL

This mpeg movie, supplements the description of water movement in the gramicidin channel as reported in Chiu, S. W., Subramaniam, S., and Jakobsson, E. 1999. Biophys. J. 76:1939-1950 The visualization was done by Elisa Ignacio, an undergraduate Bioengineering student (now just graduated) at the University of Illinois. It shows the motions over a time period of 1.2 nsec of 13 water molecules out of the 3200 in the simulated system of one gramicidin channel, 96 lipid molecules, and 3200 water molecules. These are the 13 waters that spent some time in the channel during the course of the simulation.

http://peptide.ncsa.uiuc.edu/~schiu/SWC/GA_dmpc/wat_movie.htm

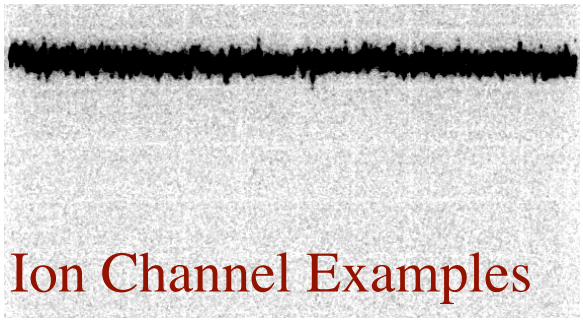

Ion Channel Examples

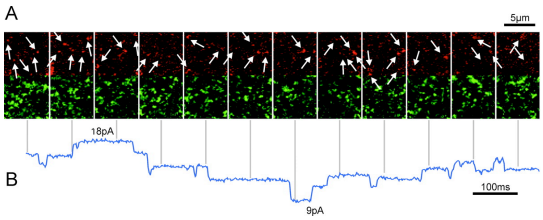

FIGURE 7 (*A*) Optical (fluorescence) images (*top: red channel, bottom: green channel*) of a bilayer containing sufficient gA-Cy3 and *p*F-Phe-gA-Cy5 to result in multiple simultaneous channel openings. FRET events (*bright dots in the red channel*) are indicated with arrows. For clarity, not all FRET events are indicated. (*B*) Simultaneous electrical recording from the same membrane. Vertical lines indicate the position of each image in the time record. The acquisition time for each image was 6 ms.

Source: Borisenko et al., 2003 Simultaneous optical and electrical recording of single gramicidin channels. Biophysical J. 84: 612-622.

Gramicidin:

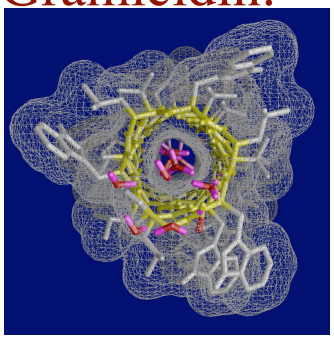

The pore passes both ions (positively charged) *and* water molecules. End to end dimer structure is most likely, although direct evidence is sparse.

http://honiglab.cpmc.columbia.edu/grasp/pictures.html

LECTURE THREE

CASE STUDY: GRAMICIDIN: MODEL ION CHANNEL

Background

Dubos (1939) isolated a crude mixture of tyrothricidine and gramicidins from Bacillus brevis (obtained from soil) and demonstrated its antibiotic activity by infecting mice with virulent pneumococci and subsequently treating them with the crude mixture, which resulted in the survival of the mice.

[Dubos, R. 1939 Studies on a bactericidal agent extracted from a soil bacillus. J. exp. Med. 70: 1-17]

Its bactericidal activity is primarily on gram-positive bacteria. Lysis is not observed. Phosphatidylethanolamine and phosphatidylserine inhibited the bactericidal activity, so there is some phospholipid specificity to its interactions with membranes.

Its toxicity to animals is high when applied systemically, so it is not useful therapeutically except in topical applications.
[Hunter Jr., FE & LS Schwartz (1967) Gramicidins. in Gottlieb & Shaw eds. Antibiotics. Vol I Springer-Verlag pp. 642-648.]

Gramicidin is described as an uncoupler. An uncoupler is a substance which 'uncouples' O_2 consumption from ATP synthesis in oxidative phosphorylation in bacteria and mitochondria.

In addition, it stimulates ATPase activity in mitochondria.

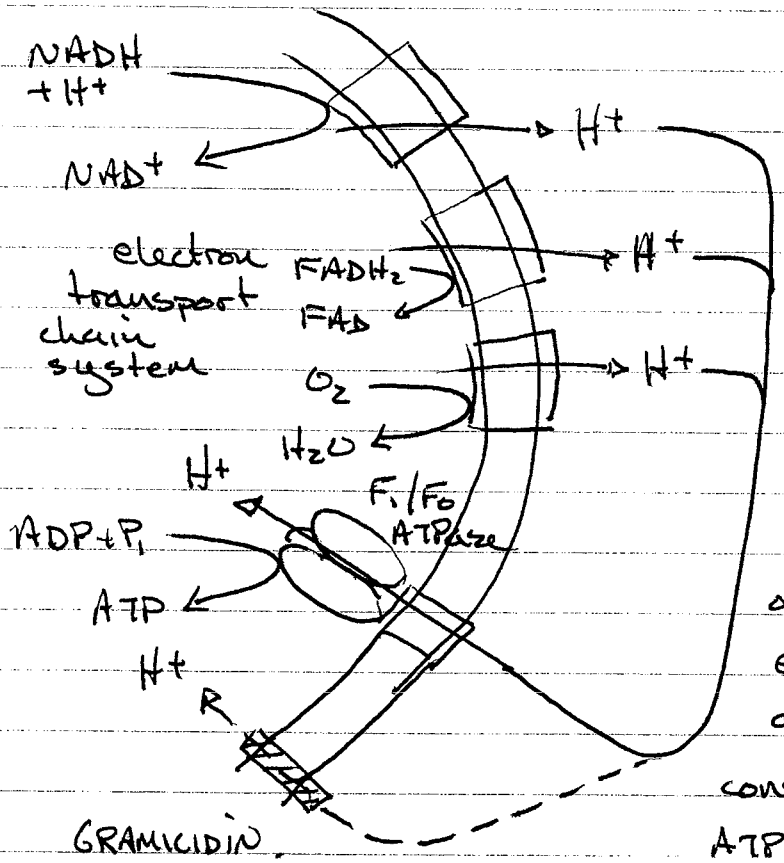

The gramicidin 'shunt' causes loss of the proton electrochemical gradient: O_2 consumption continues, ATP production stops.

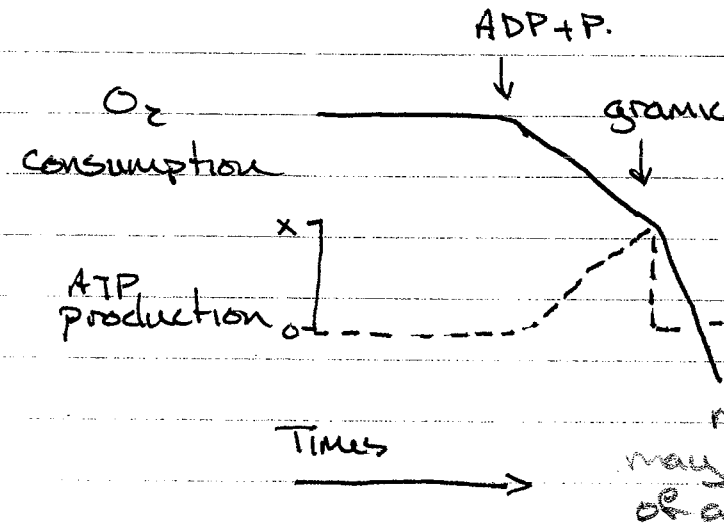

O_2 consumption no longer coupled to ATP production

note that toxic effects may involve other modes of action

Stimulation of ATPase activity.....

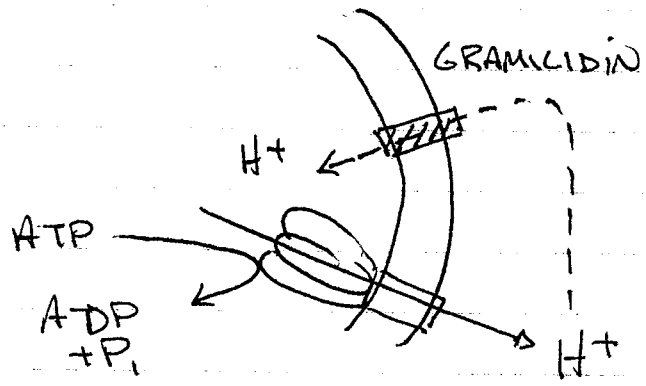

$$ATP + H^+_i \rightleftharpoons ADP + P_i + H^+_o$$

increased H^+_o & decreased H^+_i would normally 'slow' the forward rxn. Gramicidin alleviates this 'stalling', so ATPase activity increases.

When gramicidin effects on oxidative phosphorylation were first observed, the coupling of O_2 consumption to ATP synthesis by the H^+ electrochemical gradient were not known. The concept was proposed by Mitchell, and experimental evidence was obtained using isolated chloroplasts.

Acid pH

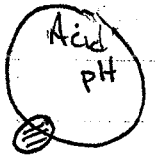

Alkaline jump:

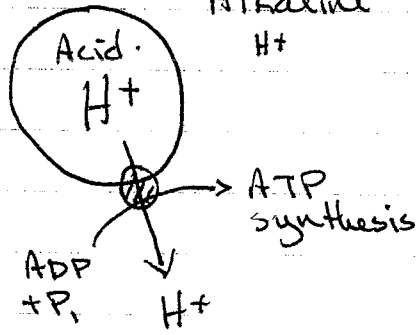

Gramicidin inhibits ATP synthesis by dissipating the H^+ gradient.

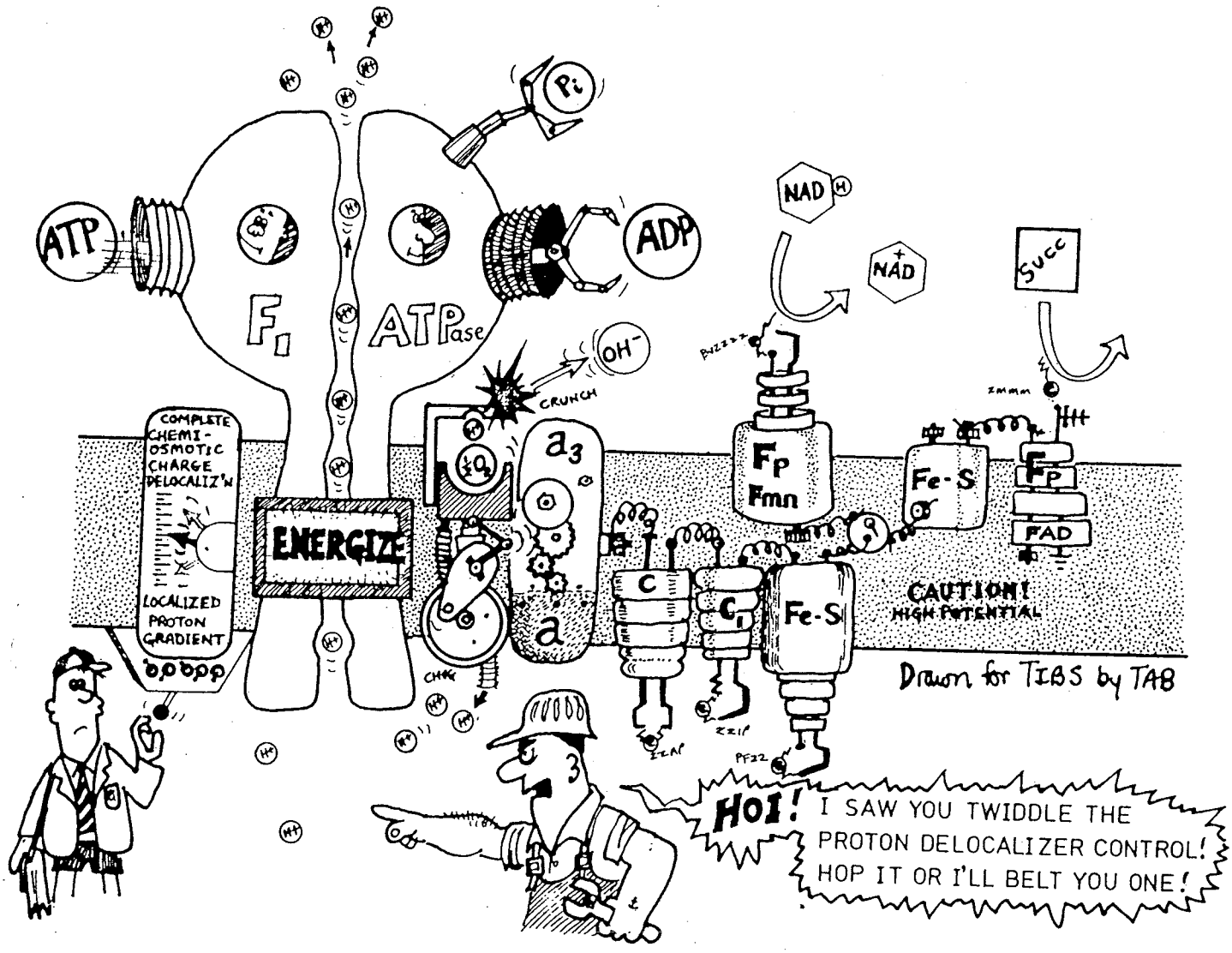

The mitochondrial respiratory chain and the ATP synthetase: the localized proton circuit/delocalized chemiosmotic debate (see p. 22)

So, what is gramicidin?

In nature, Bacillus brevis produces a mixture of gramicidins which differ in one amino acid. The linear peptide is 15 a.a. long, with alternating chiralities.

formyl - L·val - gly - L·ala - D·leu - L·ala - D·val - L·val - D·val -
L·trp - D·leu - L·xxx - D·leu - L·trp - D·leu - L·trp · ethanol-amine.

↓
trp (gramicidin A)
phe (" " B)
tyr (" " C)

Note the extreme hydrophobicity of the sequence and formyl blocking of the end N-terminus & ethanolamine at the C terminus.

Because of the hydrophobicity, it is basically insoluble in water, but can be dissolved in alcohols, organic acids etc. It partitions strongly into bilayer membranes.

The conformation in the membrane is probably:

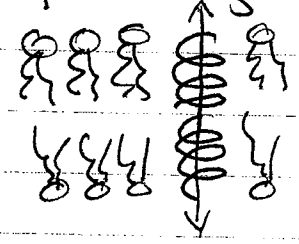

rather than:

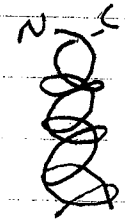

(double helix).

The Q_{10} is 1.35, corresponding to an activation energy of about 5 kcal/mol

H^+ are most mobile, consistent with the pore containing a column of hydrogen-bonded water molecules. Indeed, water does flow through the channel at about 10^8 H_2O sec^{-1}
Urea, ca 5 Å diameter, is impermeant setting an upper limit on the pore diameter.

It's important to note that gramicidin may exist in different conformational states, which have different ion conductance properties. Furthermore, it isn't necessarily a good ion channel 'model', especially because of the unnatural D-amino acids. In addition, B.A. Wallace (1990 - Gramicidin channels and pores. Ann. Rev. Biophys. Biophys. Chem. 19:127-157) points out that it isn't even clear that its antibiotic properties are due to ion leakage, rather than 'some other' bactericidal activity.

Nevertheless, it has been a gold mine for a basic characterization of ion channel conductance and selectivity.

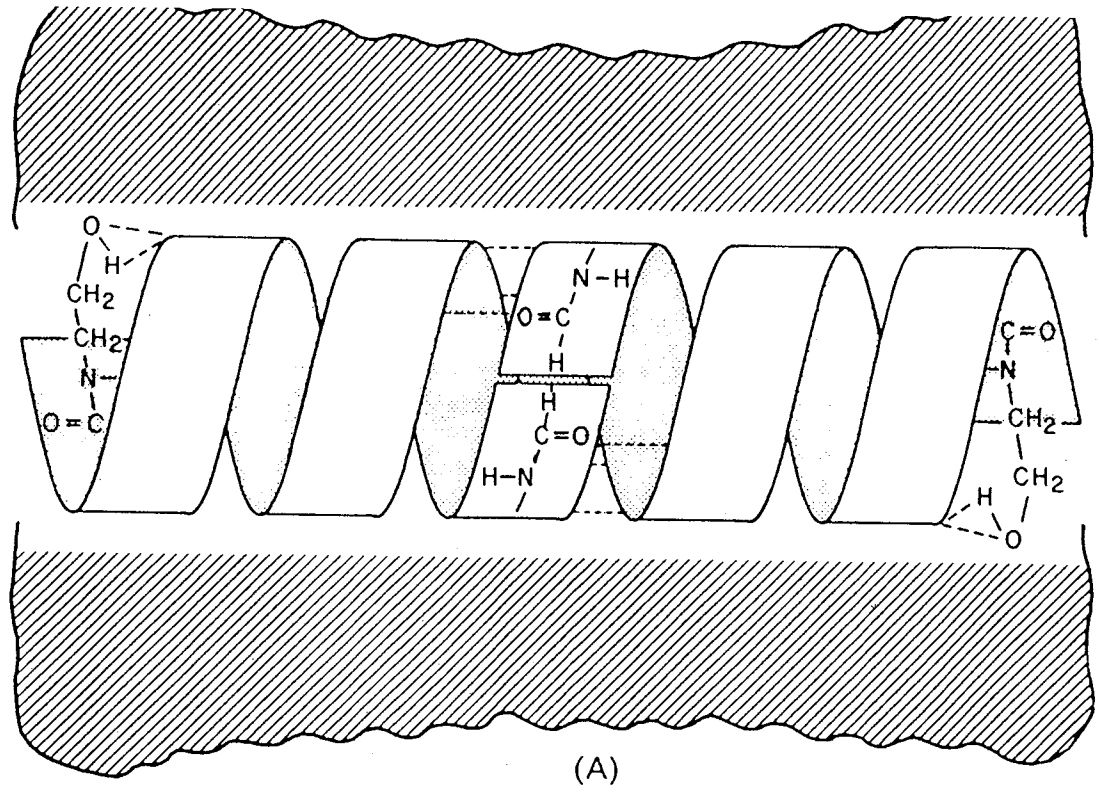

(A)

Gramicidin association/dissociation

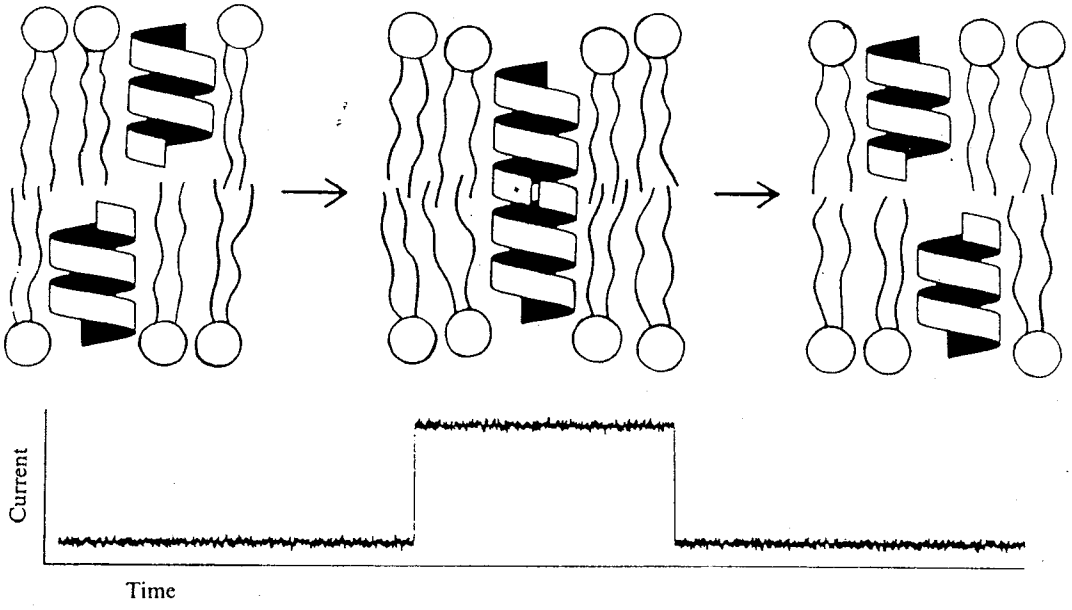

Current trace

(B)

Figure 3.34. (A) Representation of the gramicidin channel as a left-handed NH_2-terminal to NH_2-terminal $\beta^{6.3}$ helical dimer with the channel entrances at the COOH-termini. The ribbon denotes the peptide backbone, side chains the cross-hatched areas. Six H bonds are indicated at the join between the monomers (Andersen et al., 1988). (B) Requirement of a dimer for single channel conductance (conductance tracing shown; drawing from O. Andersen) illustrating the mobility of the monomers in the monolayers and the possibility of forming hybrid channels (Andersen et al., 1988).

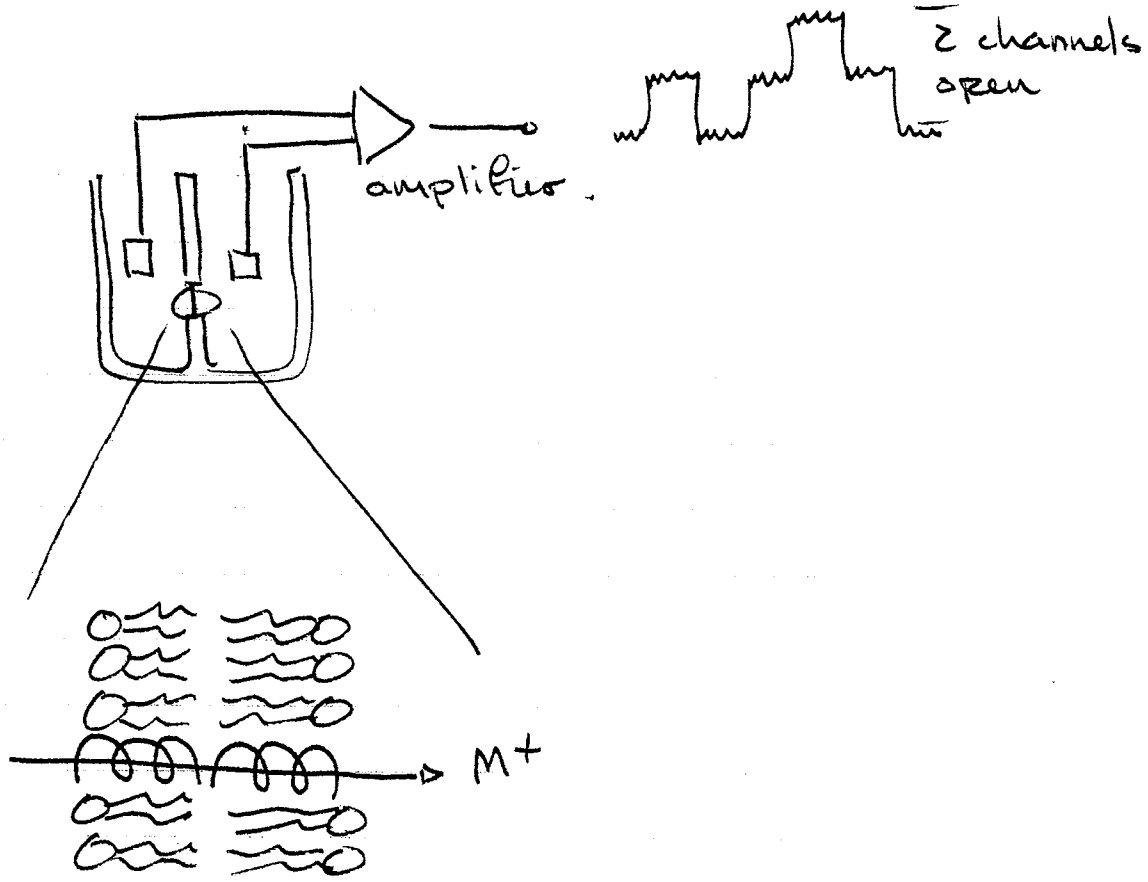

Two units of the gramicidin meet, end-to-end in the membrane, and allow passage of ions through a central pore

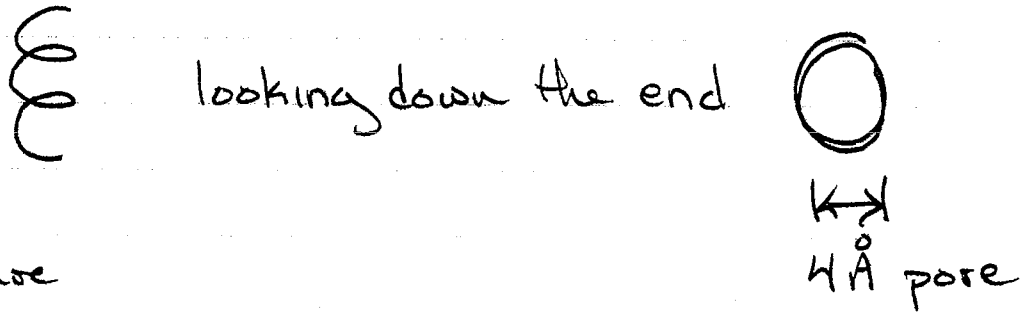

in the dimer:

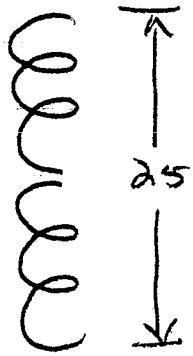

(approximate width of a membrane)

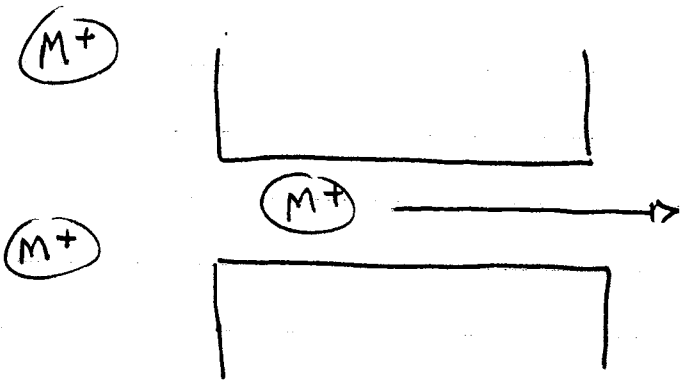

typical:

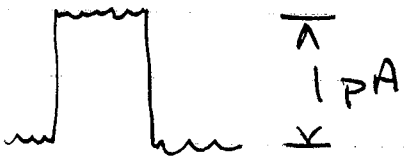

yields a conductance: ~10 pS

how many ions are flowing through the channel to yield a 1 picoampere current?

$$\underset{\text{(current)}}{I} = \underset{\text{(valence)}}{z} \cdot \underset{\text{(Faraday constant)}}{F} \cdot \underset{\text{(flux)}}{J}$$

$$\left(\frac{\text{amperes}}{\frac{\text{coulombs}}{\text{sec}}}\right) \qquad \left(\frac{\text{coulombs}}{\text{mole}}\right)\left(\frac{\text{mole}}{\text{sec}}\right)$$

$$F = 96{,}490 \ \frac{\text{coulombs}}{\text{mole}}$$

Nb coulomb is a measure of charge

$$96{,}490 \ \frac{\text{coulombs}}{\text{mole}} \cdot 6.023 \times 10^{23} \ \frac{\text{mole}}{\text{molecules}} = 10^{-19} \ \frac{\text{coulomb}}{\text{molecule}}$$

So,

$$J = \frac{I}{zF}$$

$$= \frac{10^{-9} \text{ coulombs/sec}}{+1 \ (96{,}490 \text{ coulombs/mole})}$$

$$= 1.036 \times 10^{-14} \text{ moles/sec.}$$

$$\text{or } 1.036 \times 10^{-14} \frac{\text{moles}}{\text{sec}} \cdot 6.023 \times 10^{23} \frac{\text{molecules}}{\text{mole}}$$

$$= 6.24 \times 10^{9} \text{ molecules/sec.}$$

how does this match expected flow of molecules for a pore of this diameter and length?

The answer lies in a derivation of ohm's law

$$V = IR$$

where the resistance of a geometric figure is considered: For a cylinder

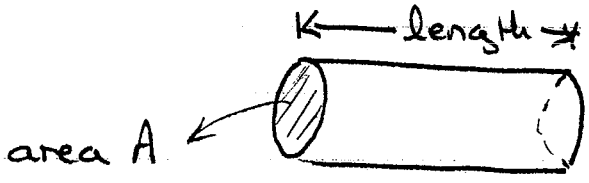

$$R = \rho \frac{l}{A}$$

where ρ is the resistivity (units ohms · cm)

For gramicidin : $l = 25\ \text{Å}$ (2.5 nm)

$A = \pi r^2 = \pi (2.5\ \text{Å})^2$

(0.25 nm).

resistivity will depend upon the ability of ions to pass current, which, ideally depends upon concentration and the diffusion coefficient. For 120 mM salt, it will be :

$$\rho = 100\ \text{ohm·cm}.$$

so

$$R_{pore} = \rho \frac{l}{\pi r^2}$$

is : $(100\ \text{ohm·cm}) \dfrac{(2.5 \times 10^{-7}\ \text{cm})}{(\pi \cdot (0.25 \times 10^{-7}\ \text{cm})^2}$

$= 12.73 \times 10^9\ \Omega$.

or $12.73\ G\Omega$

or 7.85×10^{-11} Siemens.

$78.5\ pS$

The actual value under similar conditions is about 30 pS. The overestimate could be due to ① mis-measure of pore size & length; ② limitations due to diffusion from the external medium; and ③ a lower resistivity for the ion in the pore, due to steric hindrance.

In addition, the pore may exhibit specificity for +ue or -ue ions

In the case of the gramicidin channel

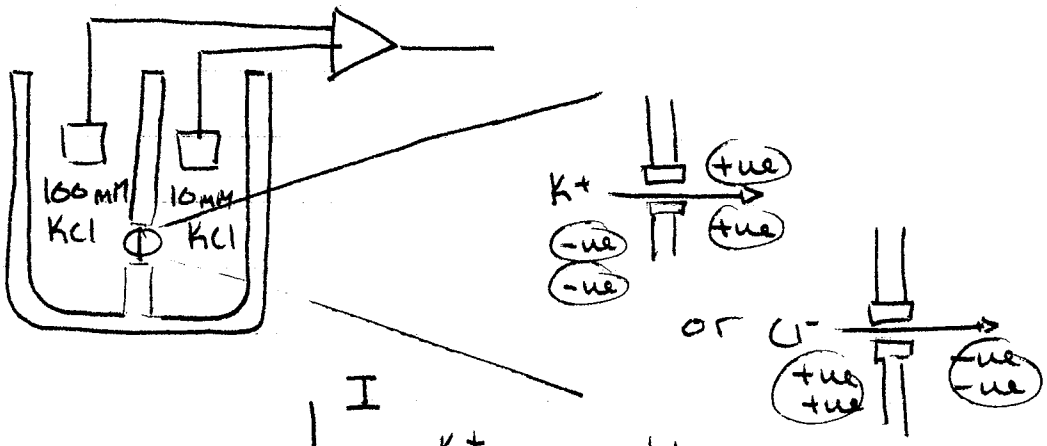

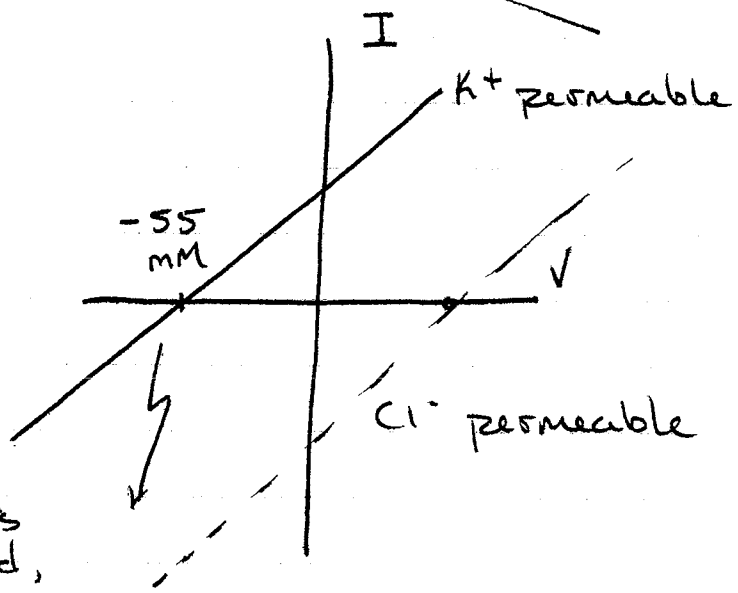

This is observed, so the gramicidin channel is +ue ion-specific

DIFFUSION POTENTIALS

When we consider conductive pathways in the membrane, such as porins and ion channels, which exhibit specificity, for example between cations (M^+) and anions (A^-), the diffusion of the ions across the membrane represents a net charge movement, and thus leads to the development of a transmembrane electrical potential.

Given two solutions (o & i) containing a completely dissociated salt: a cation c_+ and an anion, c_-, separated by a membrane. The fluxes according to the Nernst-Planck equation are:

$$J_+ = -c_+ u_+ \left[RT \frac{d \ln c_+}{dx} + zF \frac{d\psi}{dx} \right]$$

and, $$J_- = -c_- u_- \left[RT \frac{d \ln c_-}{dx} + zF \frac{d\psi}{dx} \right]$$

To solve these equations, we must invoke electroneutrality:

$$c_+^o = c_-^o = c_i^o$$

and, $$c_+^i = c_-^i = c_i^i$$

so that, $$J_- = J_+ = J_i$$

(thus, the charge imbalance that results in the development of the membrane potential is negligible compared to J_+ & J_-)

NERNST-PLANCK ELECTRONEUTRALITY: A DIGRESSION

The Nernst-Planck condition of electroneutrality results from the concept that, in most aqueous regions that are large compared to atomic dimensions, the total electrical charge carried by the cations is essentially equal in magnitude to the total electrical charge carried by the anions

That is, $\sum z_+ c_+ = \sum z_- c_-$

To yield a useful physical concept of electroneutrality, we will consider the effect of small deviations from electroneutrality for a spherical cell.

First, the physics:

net charge, $Q = C \Delta E$

(coulombs) (potential (volt))

capacitance (coulombs/volt)

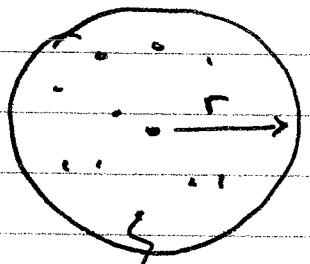

For a spherical cell of radius r

the charge $Q = \underbrace{4/3 \pi r^3}_{\text{volume of the sphere}} \cdot c \cdot F$

c: net charges at concentration c

F: Faraday constant for mole of coulomb

concentration of net charge

The capacitance C (coulombs/volt) of the sphere
(farad)

$$C = \underbrace{4\pi r^2}_{\text{area of the sphere}} \cdot C'$$

C' → capacitance per unit area. For biological cells, it is normally about $1\ \mu F/cm^2$

$\downarrow$

Farad (coulombs/volt)

Taking our charge (Q) and capacitance (C) equations for the spherical cell and inserting them into the basic equation:

$$Q = C\Delta E \rightarrow \Delta E = \frac{Q}{C}$$

$$\Delta E = \frac{4/3\,\pi r^3 \cdot c \cdot F}{4\pi r^2 C'} = \frac{rcF}{3C'}$$

or c, the concentration of net charge

$$c = \frac{\Delta E\, 3C'}{r\, F}$$

For a cell of radius 10 μm (10×10^{-4} cm) and a membrane potential of −100 mV (−0.1 Volt)

$$C = \frac{\Delta E \cdot 3 \cdot C'}{r \cdot F} \quad \left(\text{coulomb/volt}\right)$$

$$= \frac{(0.1V)(3)(10^{-6}\ F/cm^2)}{(10 \cdot 10^{-4}\ cm)(96{,}487\ \text{coulomb/mole})}$$

$$= -3 \times 10^{-9}\ \text{mole/cm}^3$$

(the negative sign indicates a net negative inside charge to create the negative inside potential)

$$= -3 \times 10^{-6}\ \text{mole/l}$$

$$= -3\ \mu M$$

In a biological cell, typical anion concentrations would be about 0.2 M, so only a minute fraction of charges must be re-distributed to create the potential.

For fluxes, if $J_+ \neq J_-$, the consequence would be a potential large enough to result in dielectric breakdown of the membrane.

Thus, we can invoke electroneutrality:

$$J_+ = J_- = J;$$

Since $J_- = J_+$ & $c_- = c_+ = c_i$ (for inside or outside)

we set $$c_+ u_+ \left[RT \frac{d\ln c_+}{dx} + zF \frac{d\psi}{dx}\right] = c_- u_- \left[RT \frac{d\ln c_+}{dx} + zF \frac{d\psi}{dx}\right]$$

Rearranging:

$$\frac{d\psi}{dx} = \left(\frac{u_+ - u_-}{u_+ + u_-}\right)\left(\frac{RT}{zF}\right)\left(\frac{d\ln c}{dx}\right)$$

which, integrating across the membrane yields:

$$\Delta\psi = \left(\frac{u_+ - u_-}{u_+ + u_-}\right)\left(\frac{RT}{zF}\right) \cdot \ln\left(\frac{c^i}{c^o}\right)$$

If one species, either the anion or cation, is impermeable across the membrane:

$$\Delta\psi = \frac{RT}{zF} \ln\left(\frac{c^i}{c^o}\right)$$

(The Nernst potential. The sign on $\Delta\psi$ will depend upon the valence, z, of the mobile ion species).

For multiple ion species (Na^+, Cl^- & K^+ in a biological context)

$$\Delta\psi = \frac{RT}{F} \ln\left[\frac{P_{Na} C^o_{Na} + P_K C^o_K + P_{Cl} C^i_{Cl}}{P_{Na} C^i_{Na} + P_K C^i_K + P_{Cl} C^o_{Cl}}\right]$$

(nb. anion is inverted)

The Goldman equation.

The sign and magnitude of $\Delta\psi$ depends upon the relative permeabilities and concentrations inside & out.

2.5 The animal cell plasma membrane as a capacitor

The outer plasma membrane of an animal cell may be considered as a capacitor in that it is a parallel-sided non-conductor layer which separates two conductors, namely the surrounding conducting aqueous fluid and the conducting fluid contained within the cell. In fact the capacitance of a typical animal cell outer plasma membrane is about $10^{-6}\,\mathrm{F\,cm^{-2}}$ or, in SI units, $10^{-2}\,\mathrm{F\,m^{-2}}$. This is in fact a very large capacitance per unit area because the thickness of the membrane d is so small. We will now make a rough estimate of the voltage difference that results from the transfer of some ions across the membrane. We take as a simple model of a cell a sphere of radius 5 micrometres containing a solution of 0.1 molar potassium chloride and surrounded by a typical animal plasma membrane. The surface area of the cell is about $3.14 \times 10^{-10}\,\mathrm{m^2}$ so that the total capacitance C of the membrane is about $3.14 \times 10^{-12}\,\mathrm{F}$. To generate an easily measured voltage of say $dV = 5$ millivolts across the membrane we would have to transfer a charge of $Q = CdV = 1.57 \times 10^{-14}\,\mathrm{C}$ across the membrane which corresponds to 9.82×10^4 univalent cations each with the elementary charge of $1.6 \times 10^{-19}\,\mathrm{C}$. But a cell with a radius of 5 micrometres and containing 0.1 molar KCl contains 3.15×10^{10} univalent potassium cations. Thus to generate an easily measured voltage across the membrane of 5 millivolts requires a change in the number of cations within the model cell of only 3 parts per million, a concentration difference far too small to be detected in any other way. This is an illustration of the strength of electric effects for, despite the fact that the membrane has a very large capacitance and thus a very large capacity to store charge with little voltage rise, the electrical effect of the transfer of the ions across the membrane is much easier to measure than any other macroscopic consequence of the transfer.

Electricity and Magnetism in Biological Systems

D. T. EDMONDS

The Clarendon Laboratory
University of Oxford

There is even discrimination between various +ve ions:

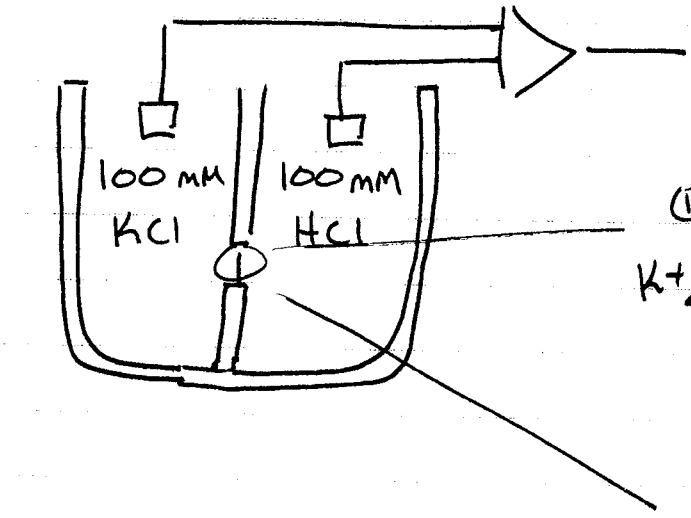

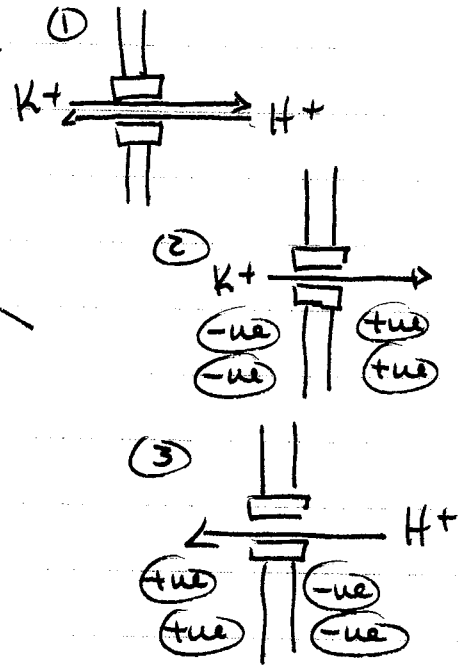

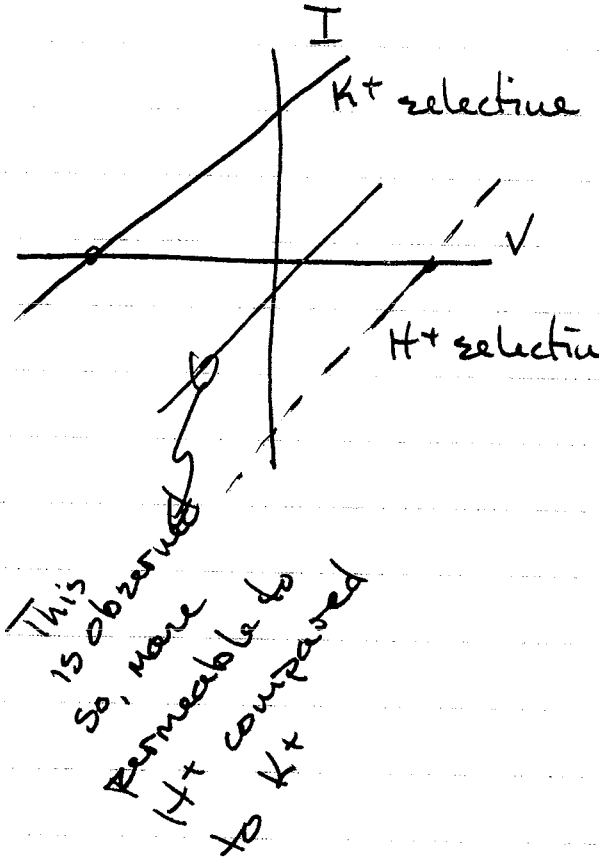

Ion Species	Permeability Ratio (relative to sodium)	Conductance Ratio (relative to sodium)	Atomic Radius (Angstroms)	Hydration Enthalpy (kcal/mole)	Mobility ([m/sec]/[V/m])
Tl	60.000,	2.100,	1.440,	. ,	7.740
H	43.000,	14.000,	. ,	. ,	36.300
NH4	6.300,	2.400,	1.480,	. ,	7.520
Cs	4.600,	2.900,	1.690,	-72.000,	8.010
Rb	3.600,	2.900,	1.480,	-79.200,	8.060
K	3.500,	1.800,	1.330,	-85.800,	7.620
Na	1.000,	1.000,	0.950,	-104.600,	5.190
Li	0.290,	0.230,	0.600,	-131.200,	4.010

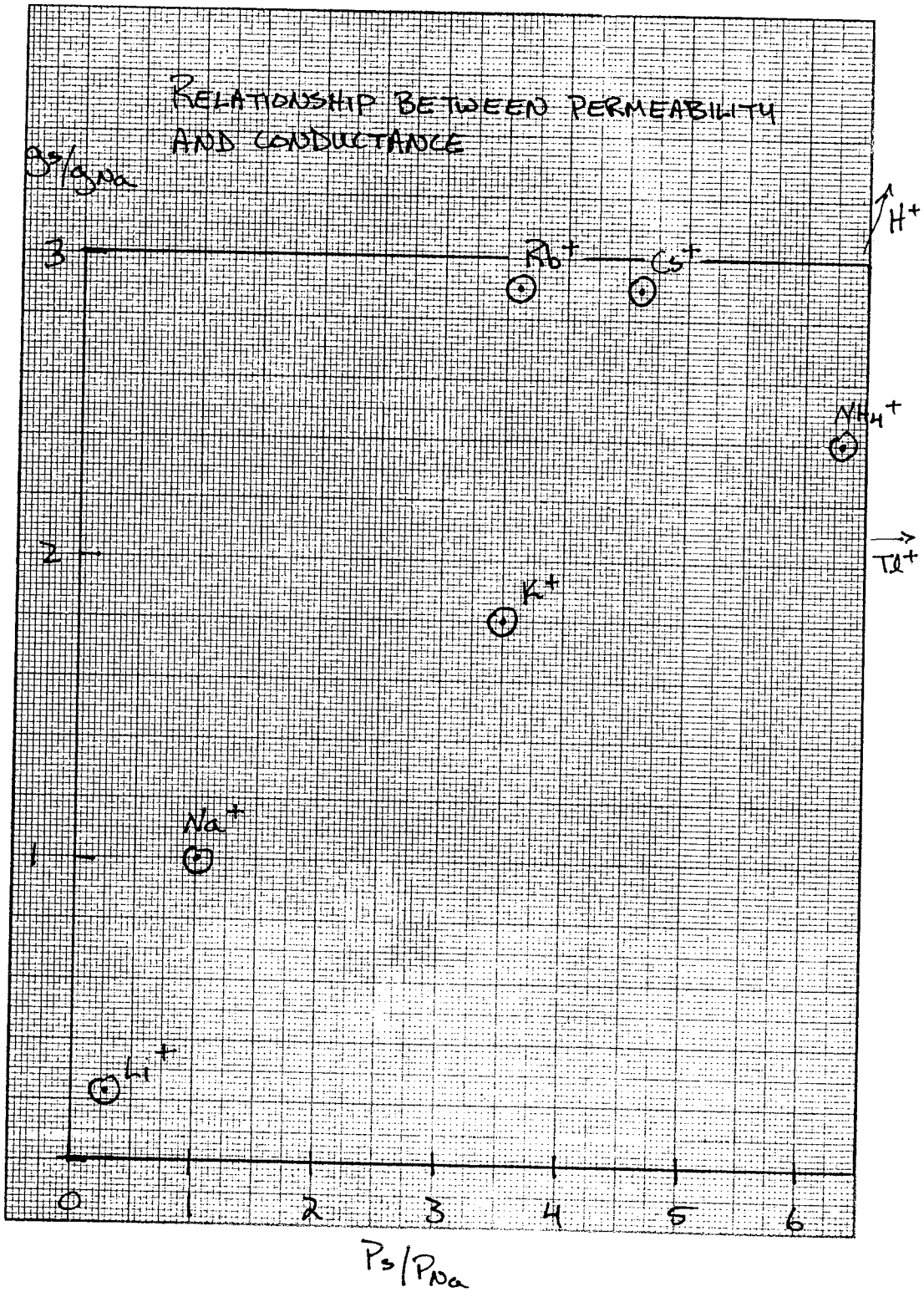
RELATIONSHIP BETWEEN PERMEABILITY AND CONDUCTANCE
g_s/g_{Na}
P_s/P_{Na}
H^+
Rb^+
Cs^+
NH_4^+
Tl^+
K^+
Na^+
Li^+
3
2
1
0
1
2
3
4
5
6

Gramicidin channel relative ion permeabilities versus conductance

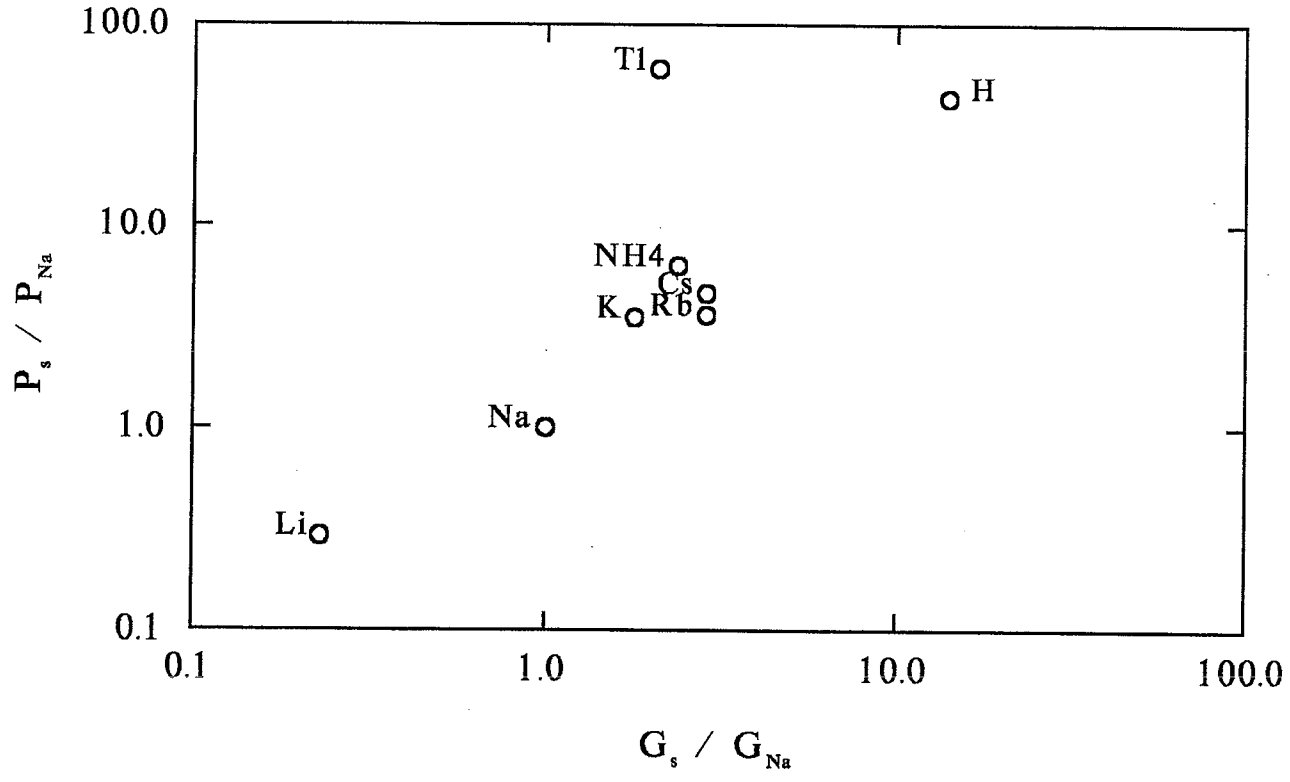

Physical Properties of Ions.

Atomic Radius.

The atomic radius is obtained by x-ray crystallography measurements of salt crystals

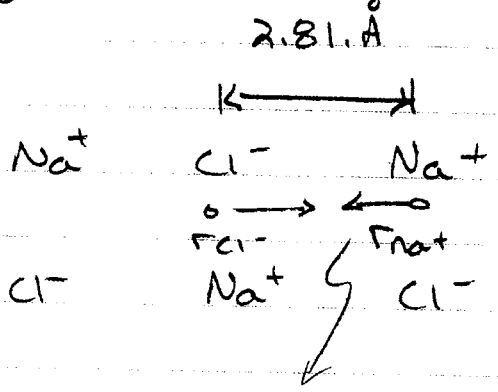

estimates of contribution by Na^+ and by Cl^- rely upon 'best guesses' of the extent to which the nuclei & electrons contribute.

Since Cl is larger (Atomic No 17, Molec. wt. 35.5) than Na (Atomic No. 11, Molec wt. 23), it contributes more:

Na	0.95 Å
Cl	1.81 Å

Charge Density

In bioinorganic chemistry, metal ions are considered to be "hard" or "soft"

hard small and less easily polarized.

→ distance is short, so e⁻ removal is difficult.

soft large and easily polarized

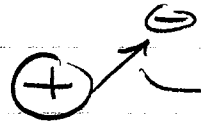

→ longer distance, so e⁻ removal is easier.

In addition, the outer electron shells will exhibit varying levels of charge density. Larger ions will have lower ⁻ densities while smaller ions will have a higher density.

All ions we deal with in membrane transport - H^+, K^+, Na^+, Ca^{2+} - are 'hard' to varying degrees. But other ions, Fe^{2+} & Cu^+, are 'softer'

Hydration

Since we are in an aqueous environment, solvation of ions is an important event, since it will change the ion's 'effective size'

The usual measure of hydration is an enthalpic one:

$$\Delta H_{hydration} = \Delta H_{gaseous\ ions \longrightarrow solution}.$$

The increase of enthalpy as a mole of free ion in vacuum is dissolved in a large volume of water

This is different from "heats of solution"

$$\Delta H_{salt \longrightarrow solution}$$

which are normally small (a few kcal/mole).

Predicted $\Delta H_{hydration}$ depends explicitly upon the radius of the ion.

$$\Delta G = \frac{z^2 e^2 N}{8\pi\varepsilon_0 r}\left(\underbrace{\frac{1}{\varepsilon_2}}_{(H_2O \sim 80)} - \underbrace{\frac{1}{\varepsilon_1}}_{(vacuum = 1)}\right)$$

e = electron charge 4.8×10^{-10} esu, N = Avogadro's No.

ε are dielectric constants $\frac{e^2 N}{8\pi\varepsilon_0} = 166$ Å kcal/mol

The actual character of the hydration shell is apparently pleiomorphic

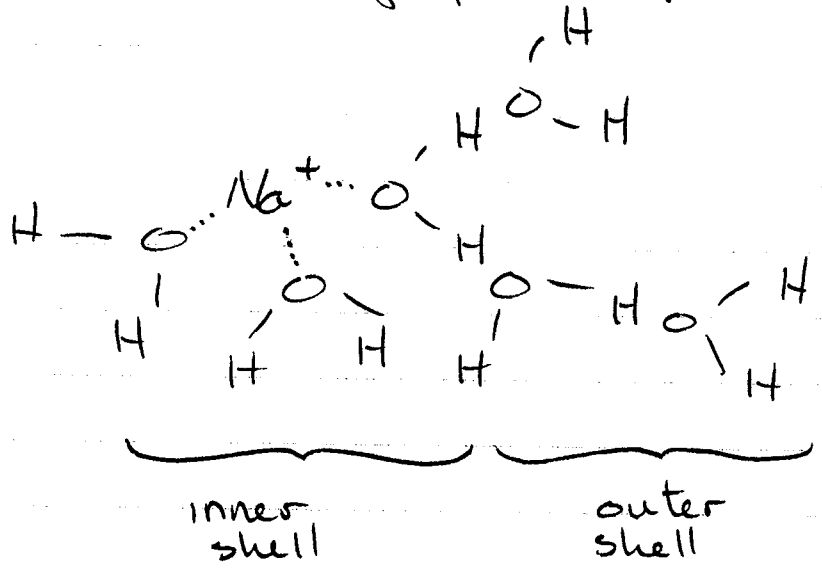

or, alternatively:

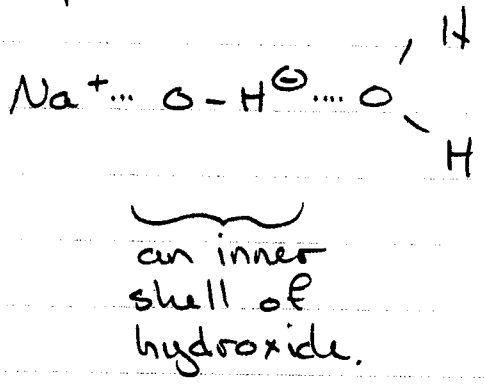

Rates of H_2O exchange between 'bound' and 'free' are fast:

	exchange rate 1st coordination sphere
Li^+	$4 \times 10^{+8}$ sec^{-1}
Na^+	$7 \times 10^{+8}$
K^+	$1 \times 10^{+9}$
Mg^{2+}	$6 \times 10^{+5}$
Ca^{2+}	$3 \times 10^{+8}$

Ion mobility versus atomic radius

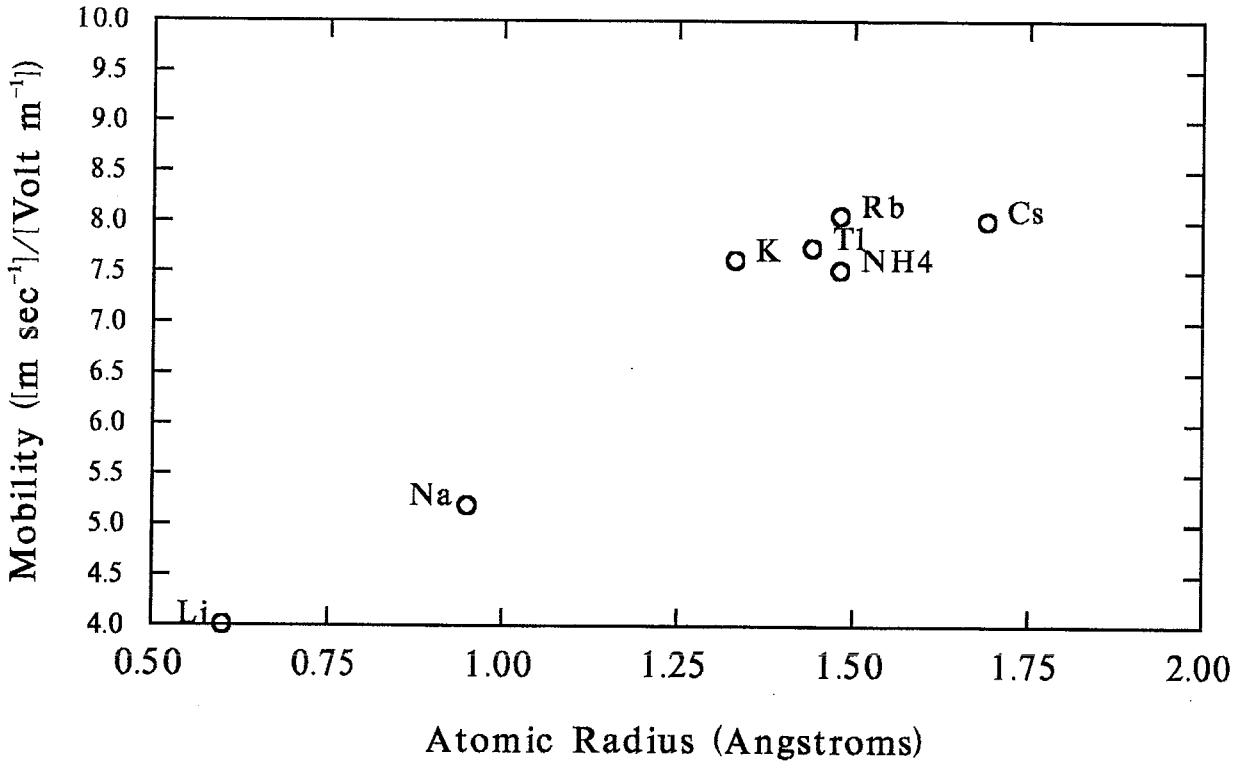

Hydration enthalpy versus atomic radius

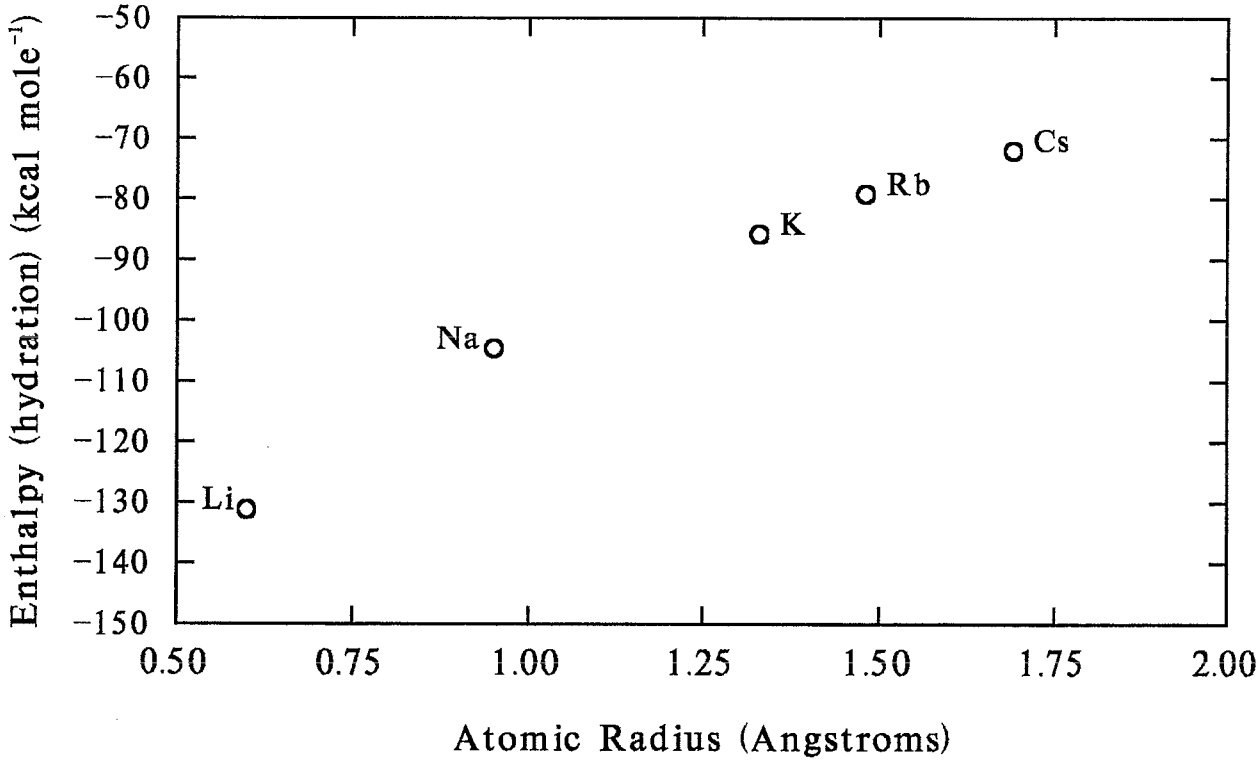

The moving-boundary method yields more accurate data on transference numbers than does the Hittorf method. Experimentally it is easier to handle. The difficulties lie in the establishment of a sharp boundary, the necessity of avoiding convection currents, and excessive heating by the current. However, once the boundary is established, the flow of current sharpens the boundary, making this a minor difficulty. The relative concentrations of the two solutes is important in maintaining a sharp boundary. The faster moving ion, M′ in this example, does not lead by more than a few angstroms, since this develops a potential difference in such a sense as to slow it down; in the steady state the two ions move with the same velocity, but M′ is always a little bit ahead of M.

The measurements of the transference number are made over a range of concentration of electrolyte; the plot of t versus $\sqrt{c}$ is linear in dilute solution and can be extrapolated to $c = 0$ to obtain the value of the transference number at infinite dilution t^0.

30–12 Equivalent Ionic Conductivities

Once measurements of transference numbers have been made, it is possible to calculate the value of the equivalent ionic conductivities of the ions, using the relations

$$\lambda_+^0 = t_+^0 \Lambda^0, \qquad \lambda_-^0 = (1 - t_+^0)\Lambda^0.$$

Values of λ_+^0 and λ_-^0 for a number of ions are given in Table 30–4.

It is interesting to compare the conductivities of the alkali metal ions:

Ion	Li^+	Na^+	K^+	Rb^+	Cs^+
λ_+^0	38.66	50.11	73.52	77.8	77.3

If we insist on the Stokes' law interpretation of these values, in analogy to Eq. (30–35) we would write

$$\lambda_+^0 = \frac{\mathscr{F} e z_+}{6\pi\eta(300) r_+}. \tag{30–42}$$

We would be forced to conclude that the radius of lithium ion is *larger* than that of cesium ion. Since the crystallographic radius of lithium is much smaller than that of cesium, this indicates a difficulty with the Stokes' law interpretation. However, we can argue that the lithium ion is large because it carries a load of water molecules with it, while the cesium ion, which has a relatively weak field to hold the water molecules to it, carries very little water. This is, in fact, correct although it does not justify the use of Stokes' law.

The transport of water by the ions was first measured by Washburn. Using the Hittorf method, a reference substance such as sugar or urea is added to the solution.

Table 30–4† Ion conductances at infinite dilution at 25°C

Cation	λ_+^0	Anion	λ_-^0
H^+	349.8	OH^-	197.8
Li^+	38.66	Cl^-	76.35
Na^+	50.11	Br^-	78.20
K^+	73.52	I^-	76.9
Rb^+	77.8	NO_3^-	71.44
Cs^+	77.3	ClO_3^-	64.6
Ag^+	61.92	BrO_3^-	55.8
Tl^+	74.7	IO_3^-	40.5
NH_4^+	73.4	ClO_4^-	67.3
$(CH_3)_4N^+$	45.0	IO_4^-	54.5
$\frac{1}{2}Mg^{2+}$	53.06	HCO_3^-	44.5
$\frac{1}{2}Ca^{2+}$	59.50	$Acetate^-$	40.9
$\frac{1}{2}Sr^{2+}$	59.46	$Benzoate^-$	32.3
$\frac{1}{2}Ba^{2+}$	63.64	$Picrate^-$	30.4
$\frac{1}{2}Cu^{2+}$	54	$\frac{1}{2}C_2O_4^{2-}$	24.0
$\frac{1}{2}Zn^{2+}$	53	$\frac{1}{2}SO_4^{2-}$	80.0

† By permission from H. S. Harned and B. B. Owen, *The Physical Chemistry of Electrolytic Solutions*. 3rd ed. Reinhold Publishing Corp., New York, 1958.

Presumably the reference substance does not move in the field, and the transport of the solvent can be calculated from the analysis of the solution in the three compartments. If a value is assumed for the number of water molecules attached to one ion, a value for the number attached to the other ion can be calculated. Presently other methods for evaluation of hydration numbers are preferred from the partial molar volume of the salt in the solution, for example. The different methods are internally consistent but often do not agree well with each other. It is generally agreed that the negative ions are not hydrated. Then the hydration numbers are, approximately: Li^+, 6; Na^+, 4; K^+, 2; Rb^+, 1. (These values have been rounded to integers.)

The data in Table 30–4 also show that the equivalent conductivities of the hydrogen ion and the hydroxyl ion are much larger than those of other ions. The very large values of the equivalent ionic conductivity observed for H^+ and OH^- have been explained on the basis of a proton jump from one species to another. For conduction by H^+ ion, we have the scheme shown in Fig. 30–9. A proton is transferred from the H_3O^+ ion to an adjacent water molecule, thereby converting the water molecule to an H_3O^+ ion. The process is repeated, the newly formed H_3O^+ ion handing on a proton to the next water molecule, and so on. The occurrence of this process leaves the water molecules in an unfavorable orientation; for the process to happen again, they must rotate through 90°. The initial stage is shown in

Ion mobility versus atomic radius

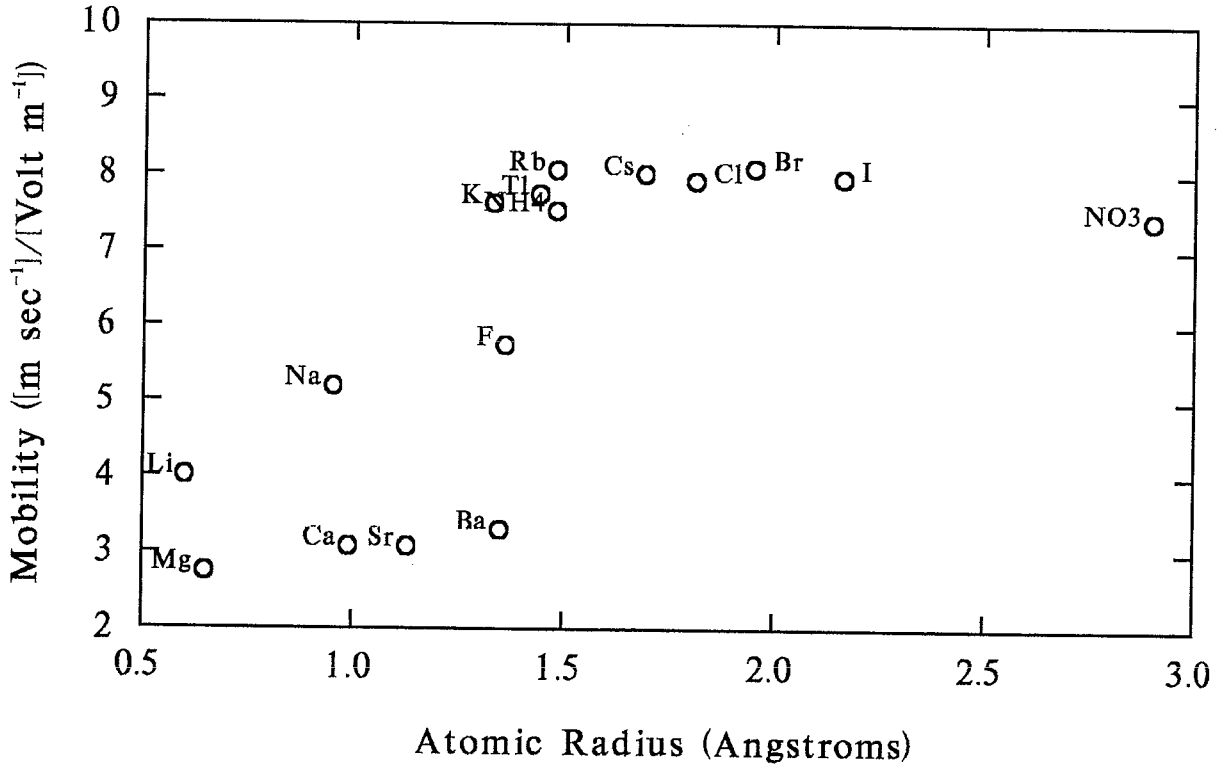

Hydration enthalpy versus atomic radius

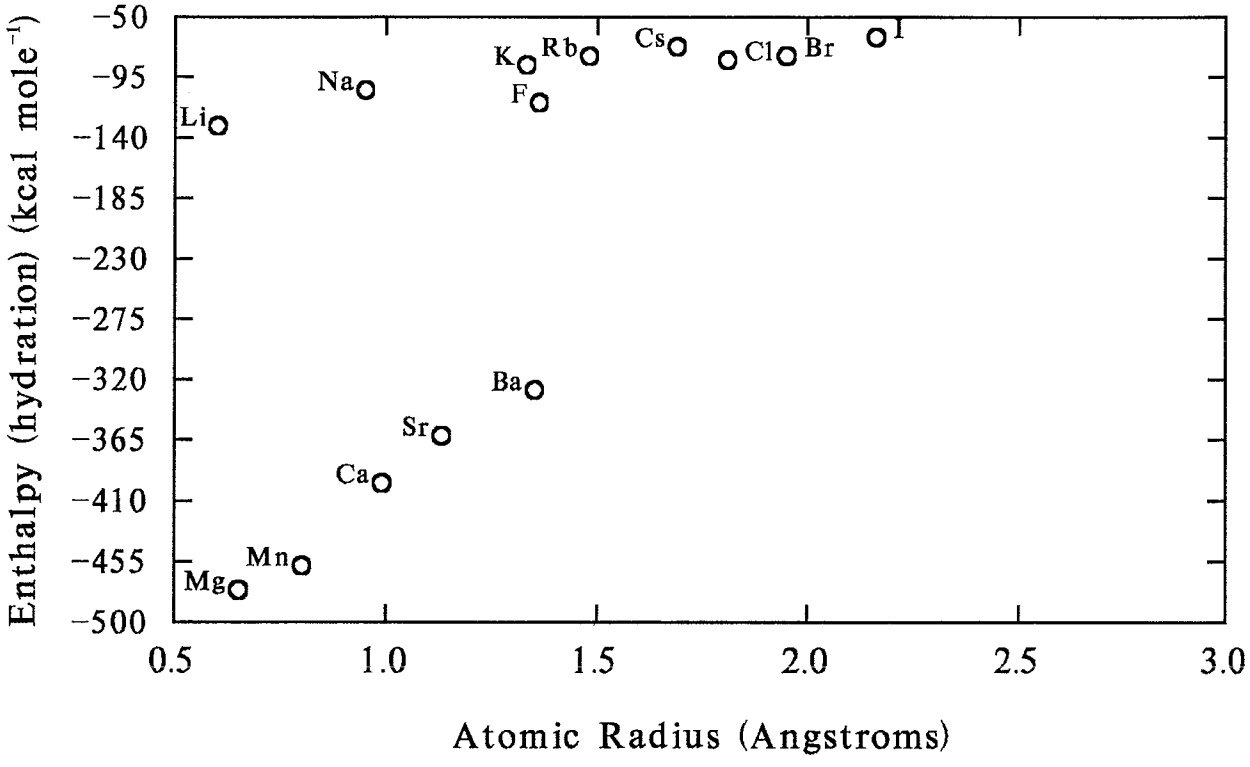

Mobility versus hydration enthalpy

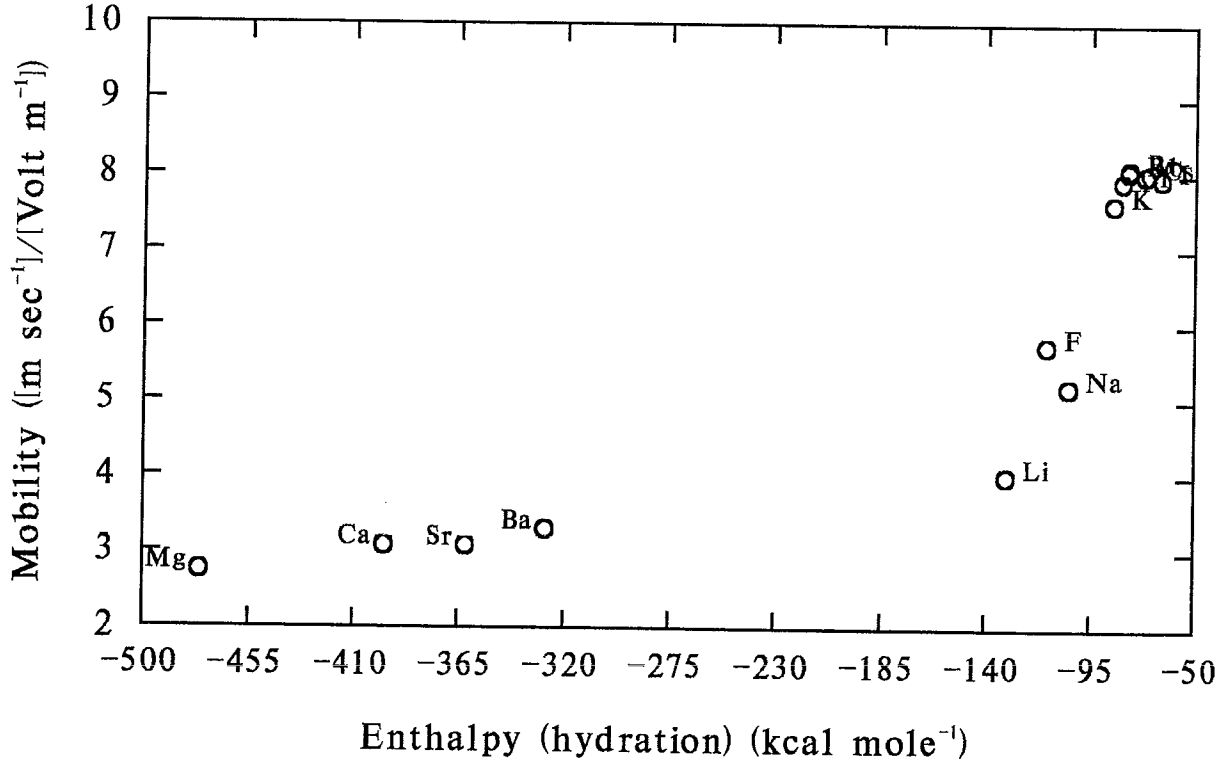

Mobility versus hydration enthalpy

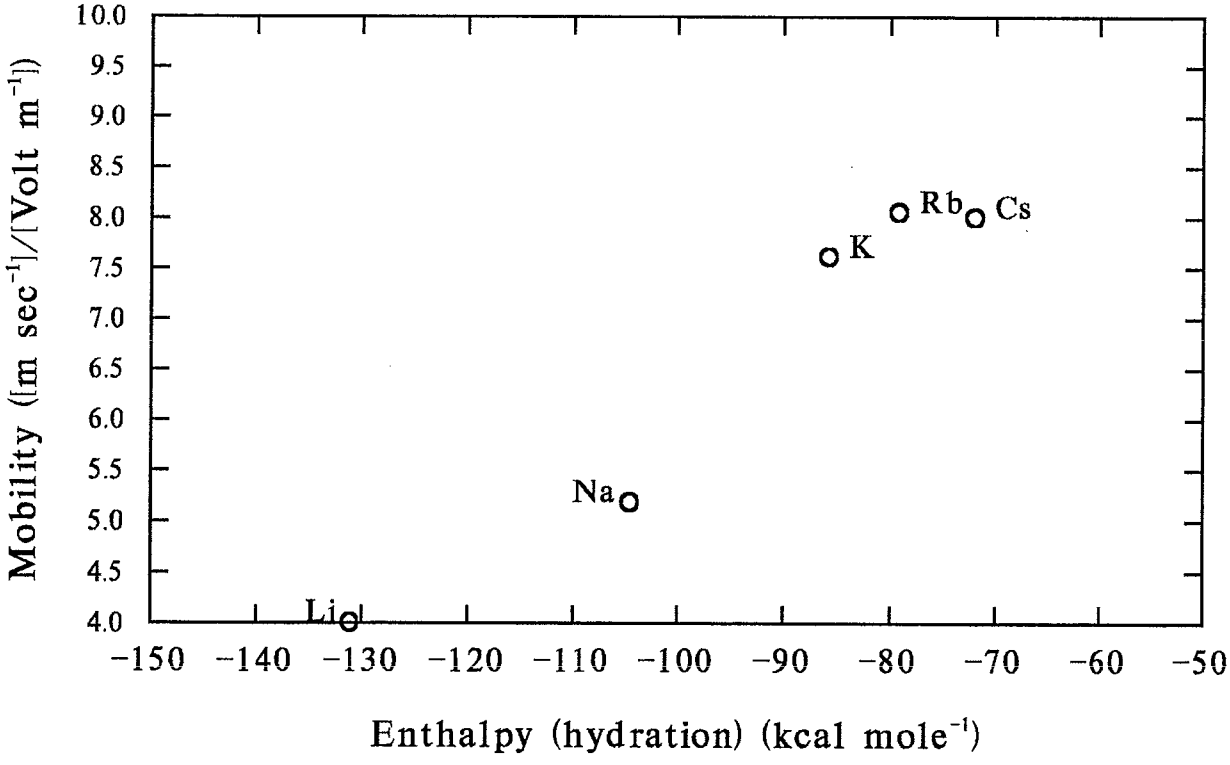

Ionic Mobility (Berg, Chapter 4)

To start, wee ned to return to a random walk:

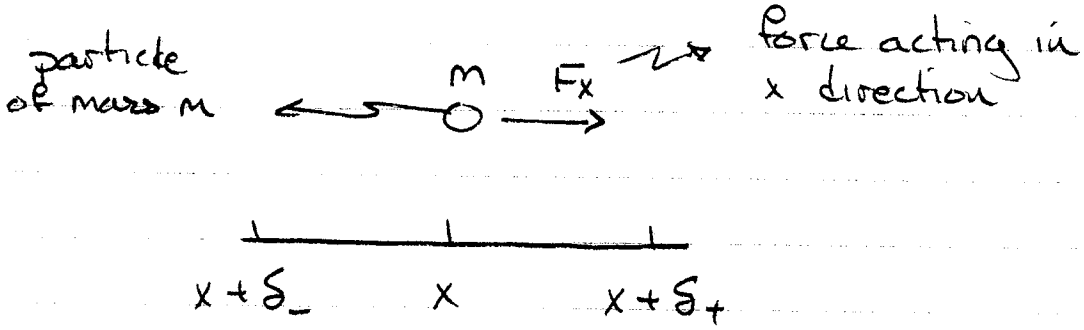

The force F_x results in an acceleration in the +ve direction, $a^{\circledast} = F_x/m$. The particle moves to the right or to the left with an initial velocity of $+v_x$ or $-v_x$ once every τ seconds

$\circledast$ units of acceleration cm sec^{-2}

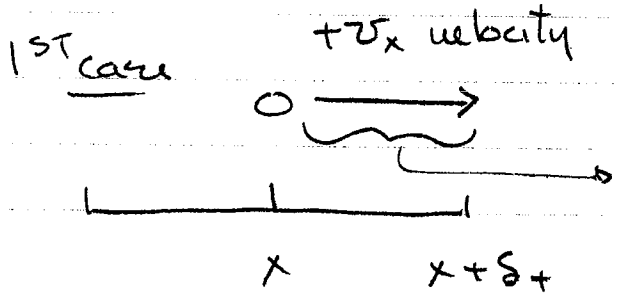

$$\delta_+ = v_x\tau + a\tau^2/2$$

distance moved due to acceleration

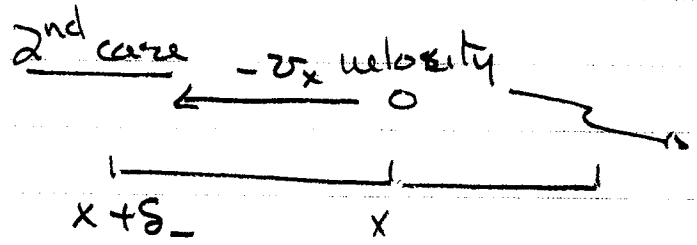

$$\delta_- = -v_x\tau + a\tau^2/2$$

If the probability that the particle goes left or right is the same: then the average displacement

$$\frac{s_+ + s_-}{2}$$

is $$\frac{\left(v_x \tau + a\tau^2/2\right) + \left(-v_x \tau + a\tau^2/2\right)}{2}$$

$v_x \tau$ cancel out: ↓

$$\frac{a\tau^2/2 + a\tau^2/2}{2}$$

↓

$$a\tau^2/2 \quad \text{(average displacement)}$$

$$v = \frac{s}{\tau}$$

and the average velocity

is $$\frac{a\tau^2/2}{\tau} = a\tau/2$$

or $$v = \frac{1}{2}\frac{F_x}{m}\tau$$

a frictional drag coefficient, f, is commonly employed:

$$v = \frac{F_x}{f} \quad \text{where } f = 2M/\tau$$

The frictional drag coefficient,

$$f = 2M/\tau$$

can be modified:

$$v^2 = \frac{\delta^2}{\tau^2}$$

$$f = \frac{2m}{\tau} \frac{\left(\frac{\delta^2}{\tau^2}\right)}{\left(\frac{\delta^2}{\tau^2}\right)}$$

$$\text{so } f = \frac{2m v^2}{\frac{\delta^2}{\tau}} = \frac{2\tau}{\delta^2} m v^2$$

$\frac{1}{\delta}$ is D.

$$\text{so } f = \frac{m v^2}{D}$$

since $mv^2 = kT$.

$$f = \frac{kT}{D} \quad \text{or} \quad D = \frac{kT}{f}$$

The conductivity, λ°, and the diffusion coefficient, D, are equivalent to mobility, simply converted:

$$\lambda^\circ = zFu$$

and $$D = \frac{RT}{F} u$$

and are directly related to ion + H_2O radius

note that λ° is the conductivity of an ionic species. In solutions:

$$\underset{\text{(salt)}}{MA} \rightleftharpoons \underset{\lambda^\circ_+}{M^+} + \underset{\lambda^\circ_-}{A^-}$$

so solution conductivity $\Lambda^\circ = \lambda^\circ_+ + \lambda^\circ_-$ at infinite dilution which is concentration dependent:

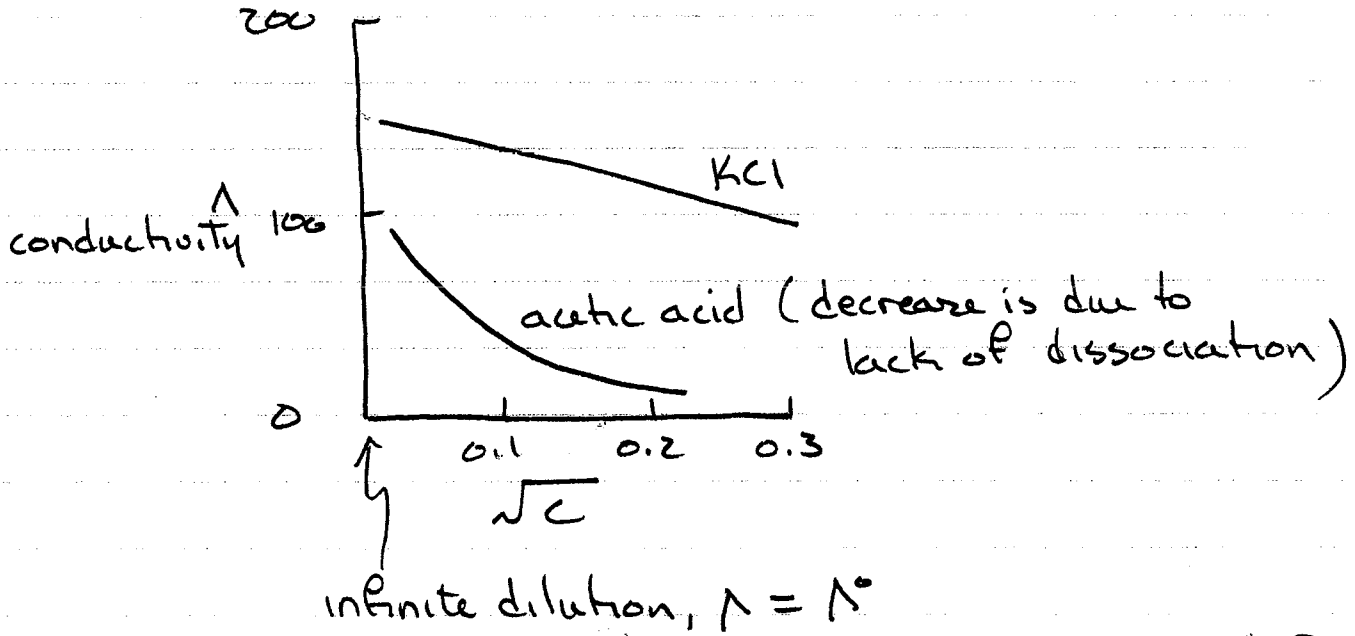

For a sphere (an ion plus its H_2O cloud)

$$f = 6\pi r \eta$$

η (eta): viscosity of solution.

r: radius of sphere

from $\frac{F_x}{f} = v$

the force, $F_x = vf$

for an ion, the force is an electrical one

$$zE\psi$$

z: valence

E: electrical charge

ψ: potential.

so $zE\psi = v\,6\pi r\eta$

The ionic mobility is defined as the $\frac{\text{velocity}}{\text{potential}} = u$

$$\frac{v}{\psi} = \frac{zE}{6\pi r\eta} = u$$

units $\left(\frac{\text{cm/sec}}{\text{volts/cm}}\right)$

r: ionic radius plus H_2O cloud.

Stoke's law plays a crucial role in understanding the forces that affect flow, especially at low Reynolds number. The derivation of Stoke's law and its relation to drag —frictional resistance to flow— will be explored in the following[1]. Stokes measured the rate of fall of spheres of various densities in media of various viscosity and found that the rate of fall followed the following relation:

$$\tfrac{2}{9}(\gamma_s - \gamma_f) = \eta v a^{-2}$$

where $(\gamma_s - \gamma_f)$ is the difference in specific weight of the sphere and the displaced fluid, η is the viscosity of the fluid, v is the velocity and a the radius of the sphere. Note that specific weight is equal to the density times the acceleration of gravity.

The net gravitational force (F) acting on the sphere as it falls is:

$$F = \tfrac{4}{3}\pi a^3(\gamma_s - \gamma_f)$$

The $(\gamma_s - \gamma_f)$ terms can be eliminated, resulting in the usual description of frictional force for a sphere, known as Stoke's Law:

$(\gamma_s - \gamma_f) = \frac{\eta v a^{-2}}{\frac{2}{9}}$ and $(\gamma_s - \gamma_f) = \frac{F}{\frac{4}{3}\pi a^3}$

$\frac{\eta v a^{-2}}{\frac{2}{9}} = \frac{F}{\frac{4}{3}\pi a^3}$, re-arranging $\frac{\eta v a^{-2}\frac{4}{3}\pi a^3}{\frac{2}{9}} = F$, simplifying $F = 6\pi\eta a v$

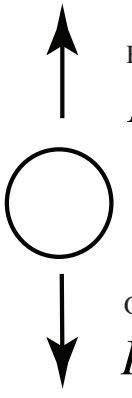

Frictional force

$$F_f = 6\pi\eta a v$$

Where the frictional and gravitational forces are balenced, the velocity reaches a steady state.

Gravitational pull

$$F_g = \tfrac{4}{3}\pi a^3 \Delta\rho g$$

[1]Dusenbery, David B. (2009) Living at Micro Scale. The unexpected physics of being small. Harvard University Press. pp. 49– 56.

Stoke's law states that frictional force increases as velocity increases[1]. There is a direct relation between Stoke's Law and the Reynolds number because Re = (ϱν*l*)/η, where ϱ is the density, ν is the velocity, *l* is the characteristic length and η is the viscosity. Velocity is usually described as a function of the drag coefficient (C_D). The graph below shows the relation between the drag coefficient and the Reynolds number[2]. At low Reynolds number —where Stoke's Law applies— the relation is linear, and predicted by Stoke's Law to be $C_D = 24/Re$. At high Reynolds number ($Re>10^3$), the relation between the drag coefficient and the frictional force is more complex: $C_D = F_f / (0.5\varrho v^2 A)$, where ϱ is the density, v^2 is the velocity squared and A is the frontal area of the object.

$$F_f = 6\pi\eta a v$$

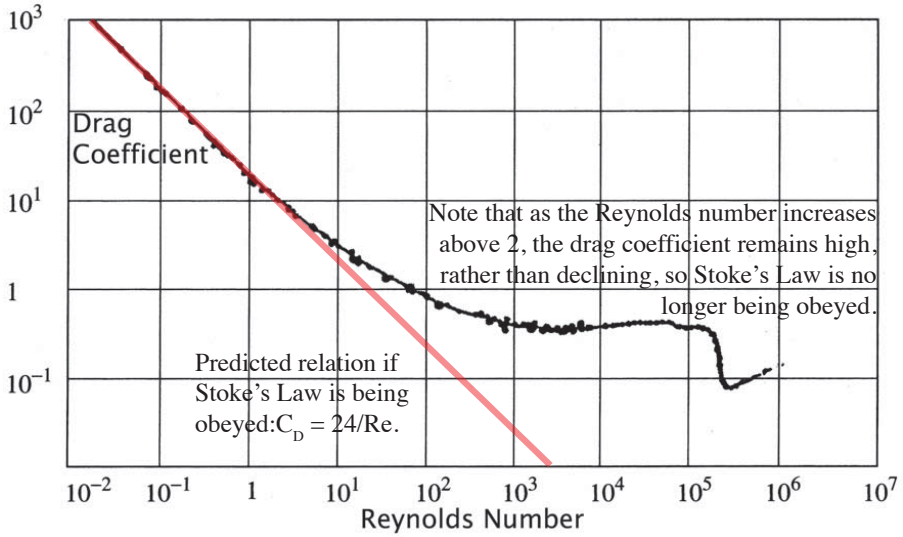

We can carry the presentation one step further, focussing on high Reynolds number, and consider the terminal velocity of an object free-falling in air:

$$V_{\text{terminal}} = \sqrt{\frac{2mg}{\rho A C_D}}$$

Terminal velocity is where the drag force (F_f) is equal to the 'downward' force of gravity (*mg*). You should be able to assess the terminal velocity at low Reynolds number by the same analytical approach.

[1]Dusenbery, David B. (2009) Living at Micro Scale. The unexpected physics of being small. Harvard University Press. pp. 49– 56.

[2]Barenblatt, G. I. (2003) Scaling. Cambridge University Press. page 41.

TABLE 1. LIMITING EQUIVALENT CONDUCTIVITIES, ELECTRIC MOBILITIES, AND DIFFUSION COEFFICIENTS OF IONS AT 25°C

Ion	$\lambda^0 = zFu$ [(S/cm)/(equiv/cm^3)]	u [10^{-4} (cm/s)/(V/cm)]	$D = RTu/F$ (10^{-5} cm^2/s)
H^+	349.8	36.25	9.31
Li^+	38.7	4.01	1.03
Na^+	50.1	5.19	1.33
K^+	73.5	7.62	1.96
Rb^+	77.8	8.06	2.07
Cs^+	77.3	8.01	2.06
Tl^+	74.7	7.74	1.98
NH_4^+	73.6	7.52	1.96
$CH_3NH_3^+$	58.7	6.08	1.56
TMA^+	44.9	4.65	1.19
TEA^+	32.7	3.39	0.87
Mg^{2+}	53.0	2.75	0.71
Ca^{2+}	59.5	3.08	0.79
Sr^{2+}	59.4	3.08	0.79
Ba^{2+}	63.6	3.30	0.85
F^-	55.4	5.74	1.47
Cl^-	76.4	7.92	2.03
Br^-	78.1	8.09	2.08
I^-	76.8	7.96	2.04
NO_3^-	71.5	7.41	1.90
Acetate	40.9	4.24	1.09
SO_4^{2-}	80.0	4.15	1.06

Conductivities from Robinson and Stokes (1965).

TABLE 4. PAULING RADII AND IONIC HYDRATION ENERGIES

Atom or group	Radius (Å)	$\Delta H°_{hydration}$ (kcal/mol)
H^+	—	−269
Li^+	0.60	−131
Na^+	0.95	−105
K^+	1.33	−85
Rb^+	1.48	−79
Cs^+	1.69	−71
Tl^+	1.40	—
Mg^{2+}	0.65	−476
Ca^{2+}	0.99	−397
Sr^{2+}	1.13	−362
Ba^{2+}	1.35	−328
Mn^{2+}	0.80	−458
Co^{2+}	0.74	−502
Ni^{2+}	0.72	−517
Zn^{2+}	0.74	−505
F^-	1.36	−114
Cl^-	1.81	−82
Br^-	1.95	−79
I^-	2.16	−65
H	1.20	—
Methyl	2.0	—
N	1.5	—
O	1.40	—

Radii from Pauling (1960). Standard enthalpies of hydration at 25°C are taken from Edsall and McKenzie (1978), who also give entropies and free energies of hydration.

Permeability (circles) and conductance (triangles) ratios versus mobility

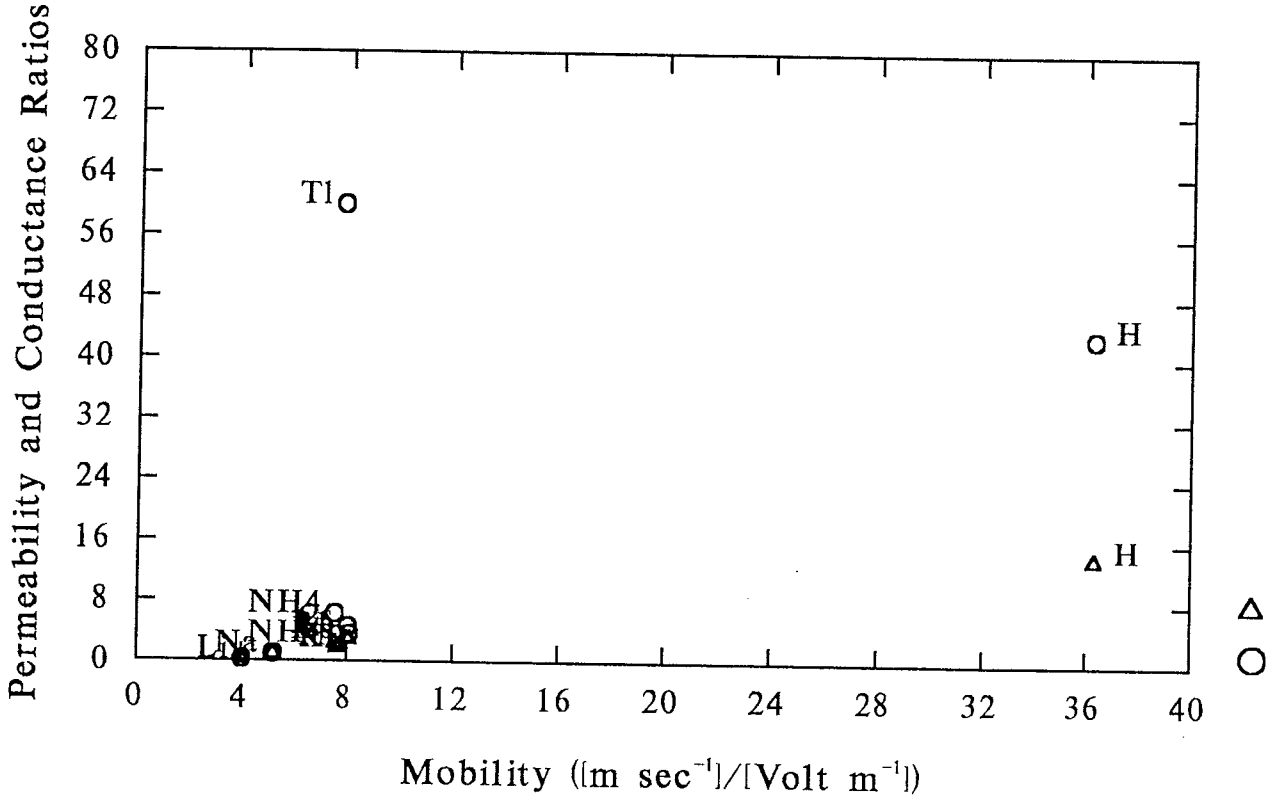

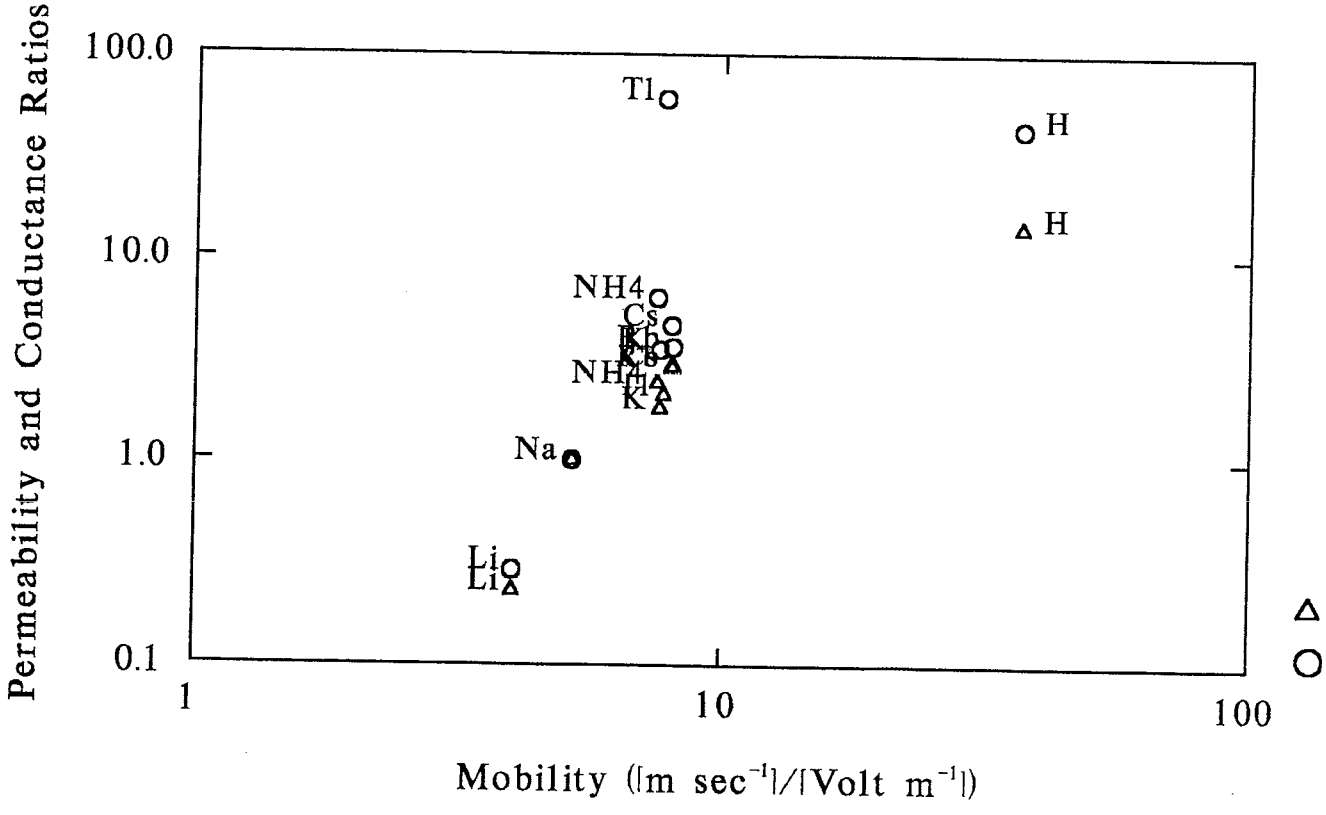

4404. Gougerotin. *1-(4-Amino-2-oxo-1(2H)-pyrimidinyl)-1,4-dideoxy-4-[D-2-[2-(methylamino)acetamido]hydracrylamido]glucopyranuronamide;* 1-[4-deoxy-4-(sarcosyl-D-seryl)amino-β-D-glucopyranuronamide]cytosine; aspiculamycin; asteromycin. $C_{16}H_{25}N_7O_8$; mol wt 443.43. C 43.34%, H 5.68%, N 22.11%, O 28.87%. Antibiotic substance from *Streptomyces gougerotii:* Kanzaki *et al., J. Antibiot.* **15A**, 93 (1962). Identity with asteromycin: Ikeuchi *et al., ibid.* **25**, 548 (1972). Structure: Iwasaki, *Yakugaku Zasshi* **82**, 1358 (1962). Revised structure: Fox *et al., Tetrahedron Letters* **1968**, 6029; Watanabe *et al., Chem. Pharm. Bull.* **17**, 416 (1969). Total synthesis: *eidem, J. Am. Chem. Soc.* **94**, 3272 (1972); Lichtenthaler *et al., Tetrahedron Letters* **1975**, 3527. Identity with aspiculamycin: Lichtenthaler *et al., ibid.* **1975**, 665. Mechanism of action study: J. C. Lacal *et al., J. Antibiot.* **33**, 441 (1980). *Reviews:* Clark in *Antibiotics,* **vol. 1**, D. Gottlieb, P. D. Shaw, Eds. (Springer-Verlag, New York, 1967) pp 278-282; Yukioka, *ibid.* **vol. 3**, J. W. Corcoran, F. E. Hahn, Eds. (1975) pp 448-458.

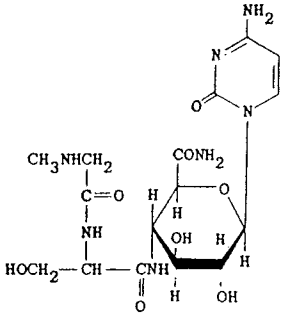

Needles, mp 211-217° (dec). $[\alpha]_D^{27}$ +53° (c = 0.8). uv max (water): 267, 235 nm (ε 9400, 9300); in 0.1 *N* HCl: 275 nm (ε 13,600); in 0.1 *N* NaOH: 267 nm (ε 9800). LD_{50} in mice: 57 mg/kg i.v., Kanzaki *et al., loc. cit.*

THERAP CAT: Antibacterial; antineoplastic.

4405. Gramicidin(s). Gramicidin D (Dubos); linear gramicidins; Gramoderm. Polypeptide antibiotic complex first isolated from the mixture tyrothricin *(q.v.)* along with tyrocidine *(q.v.)* from cultures of *Bacillus brevis:* Dubos, Hotchkiss, *J. Exp. Med.* **73**, 629 (1941); *eidem, J. Biol. Chem.* **141**, 155 (1941). Commercial extraction: Baron, U.S. pat. **2,534,541** (1950 to Penick). Commercial preparation is a mixture of the four components, gramicidin A, B, C, and D, comprising about 87.5, 7.1, 5.1, 0.3 percent resp: Gross, Witkop, *Biochemistry* **4**, 2495 (1965). Each of the components A, B, and C consist of 2 chains, one with valine in position 1, comprising 80-95% of the component, and the other with isoleucine in position 1. Structure, characterization, and synthesis of valine- and isoleucine- gramicidin A: Sarges, Witkop, *J. Am. Chem. Soc.* 86, 1862 (1964); **87**, 2011, 2020 (1965); Bauer *et al., Biochemistry* **11**, 3266 (1972). Structure of gramicidin B: Sarges, Witkop, *J. Am. Chem. Soc.* **87**, 2027 (1965); of gramicidin C: *eidem, Biochemistry* **4**, 2491 (1965). Synthesis of valine-gramicidin B and C: K. Noda, E. Gross in *Chemistry and Biology of Peptides, Proc. 3rd Am. Peptide Symp.,* J. Meienhofer Ed. (Ann Arbor Science Publishers, Michigan, 1972) pp 241-250. *Review:* Hunter, Schwartz, "Gramicidins" in *Antibiotics* I, S. Gottlieb, P. Shaw, Eds. (Springer-Verlag, New York, 1967) pp 642-648. Comprehensive description: G. A. Brewer in *Analytical Profiles of Drug Substances* **vol. 8**, K. Florey, Ed. (Academic Press, New York, 1979) pp 179-218.

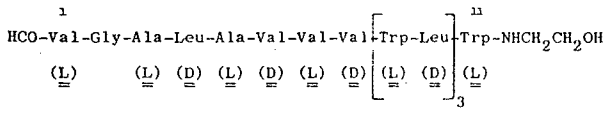

valine-gramicidin A

Spear-shaped or lenticular platelets, mp 229-230°. Almost insol in water (0.6 mg/100 ml). Soluble in the lower alcohols, acetic acid, pyridine. Moderately sol in dry acetone and dioxane. Practically insol in ether, hydrocarbons. Tends to form colloidal suspensions in water.

THERAP CAT: Antibacterial.

THERAP CAT (VET): Antimicrobial.

4406. Gramicidin S. Gramicidin S (Soviet); gramicidin C (Soviet). $C_{60}H_{92}N_{12}O_{10}$; mol wt 1141.49. C 63.13%, H 8.12%, N 14.72%, O 14.02%. Cyclic decapeptide antibiotic produced by a strain of *Bacillus brevis.* Isoln: Gause *et al., Compt. Rend. Acad. Sci. USSR* **43**, 217 (1944), *C.A.* **39**, 1195 (1945); Gause, Brazhnikova, *Lancet* **247**, 715 (1944). More closely related to tyrocidines, *q.v.*, in biological and chemical properties than to true gramicidins, *q.v.* Structure: Synge, *Biochem. J.* **39**, 363 (1945); Consden *et al., ibid.* **40**, xliii (1946); **41**, 596 (1947); Battersby, Craig, *J. Am. Chem. Soc.* **73**, 1887 (1951); Erlanger, Goode, *Nature,* **174**, 840 (1954). Synthesis: Schwyzer, Sieber, *Helv. Chim. Acta* **40**, 624 (1957); Waki, Izuniya, *Bull. Chem. Soc. Japan* **40**, 1687 (1967). Solid phase synthesis: Losse, Neubert, *Tetrahedron Letters* **1970**, 1267; M. Ohno *et al., J. Am. Chem. Soc.* **93**, 5251 (1971). Improved synthesis via a linear pentapeptide: Y. Minematsu *et al., Tetrahedron Letters* **1980**, 2179; via a linear decapeptide: T. Mukaiyama *et al., Chem. Letters* **1981**, 1367. Industrial procedure: **Brit. pat. 836,725** (1960 to Ciba). *Review:* Y. A. Ovchinnikov, V. T. Ivanov, "The Cyclic Peptides: Structure, Conformation, and Function" in *The Proteins* **vol. V**, H. Neurath, R. L. Hill, Eds. (Academic Press, New York, 3rd ed., 1982) pp 547-555.

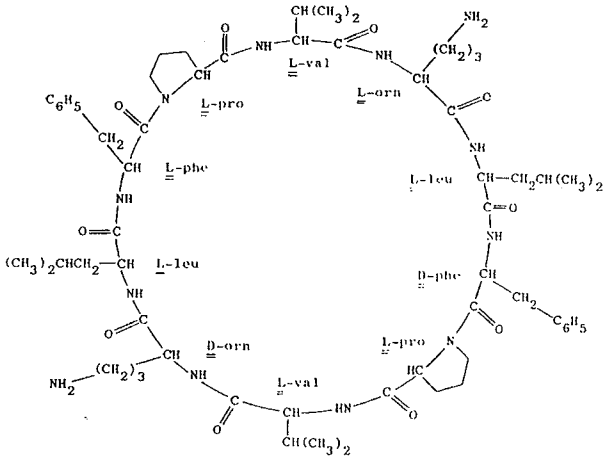

Hydrochloride, $C_{60}H_{92}N_{12}O_{10}.2HCl$, prisms from ethanol + aq HCl, dec 277-278°. $[\alpha]_D^{24}$ −289° (c = 0.43 in 70% ethanol). Absorption spectrum: Schwyzer, Sieber, *loc. cit.* Freely sol in alcohol; slightly sol in acetone; practically insol in water, acids, alkalies. LD_{50} in rats: 17 mg/kg i.p., *RTECS* **Vol. I**, R. J. Lewis, R. L. Tatken, Eds. (1979) p 723.

THERAP CAT: Topical antimicrobial.

4407. Gramine. *N,N-Dimethyl-1H-indole-3-methanamine; 3-(dimethylaminomethyl)indole;* Donaxine. $C_{11}H_{14}N_2$; mol wt 174.24. C 75.82%, H 8.10%, N 16.08%. In chlorophyll-deficient mutants of barley: Euler *et al., Z. Physiol. Chem.* **217**, 23 (1933). In the Asiatic reed *Arundo donax* L., *Gramineae:* Orechoff, Norkina, *Ber.* **68**, 436 (1935). From *Acer saccharinum* L. (the Silver Maple) and *A. rubrum* L., *Aceraceae:* Pachter *et al., J. Org. Chem.* **24**, 1285 (1959); Pachter, *J. Am. Pharm. Assoc., Sci. Ed.* **48**, 670 (1959). Synthesis: Kühn, Stein, *Ber.* **70**, 567 (1937). Biosynthesis from tryptophan in barley: Bowden, Marion, *Can. J. Chem.* **29**, 1037 (1951); O'Donovan, Leete, *J. Am. Chem. Soc.* **85**, 461 (1963); Gower, Leete, *ibid.* 3683; *see also* Gross *et al., Tetrahedron Letters* **1971**, 4047.

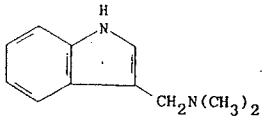

Shiny, flat needles or plates from acetone, mp 138-139°. Absorption spectrum: Kanakoa *et al., Chem. Pharm. Bull.*

One interesting aspect of research on gramicidins is the attempts to use them as 'bio-sensors'. This is a recent area of research with a very applied aspect to it: to develop highly sensitive 'sensors' for a variety of substances.

The concept begins with the awareness that a single molecular event, channel opening, causes a high gain response: ion flows at 10^5 to 10^9 molecules per second. The overall amplification is therefore 10^5 to 10^9. The problem applied scientists face is how to control 'gating' of the channel.

In 'natural' situations, ligand binds to a channel, causing it to open. To 'mimick' this process, Cornell et al. (1999) used antibodies ~~co~~-linked to gramicidin.

[Cornell, BA, VLB Braach-Maksvytis, LG King, PDJ Oman, B Raguse, L Wieczorek & RJ Pace 1999 The gramicidin-based biosensor: a functioning nano-machine. Novartis Found. Symposium. Vol. 225 pp 231-254.]

Tethered species

1. 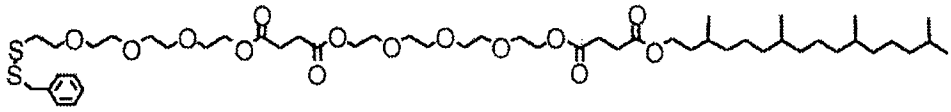

2. 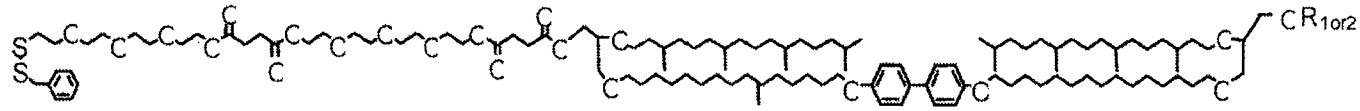

3. 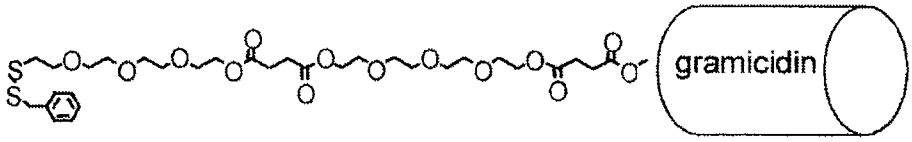

Mobile species

4. 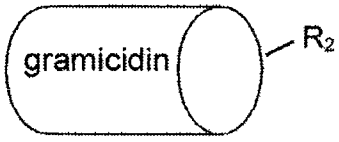

5. 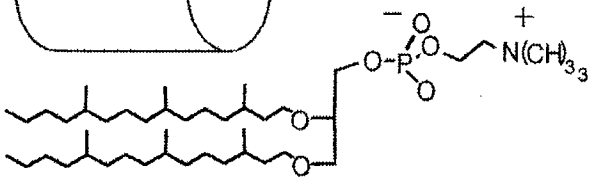

6. 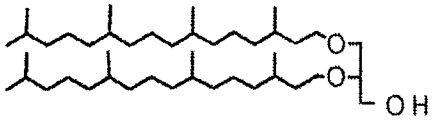

Where for both the mobile and tethered species

$R_1 = H$

$R_2 =$ 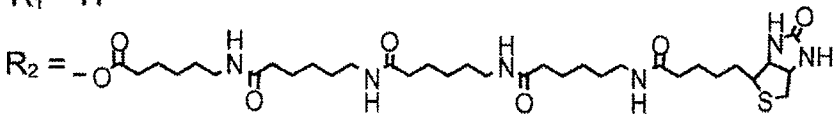

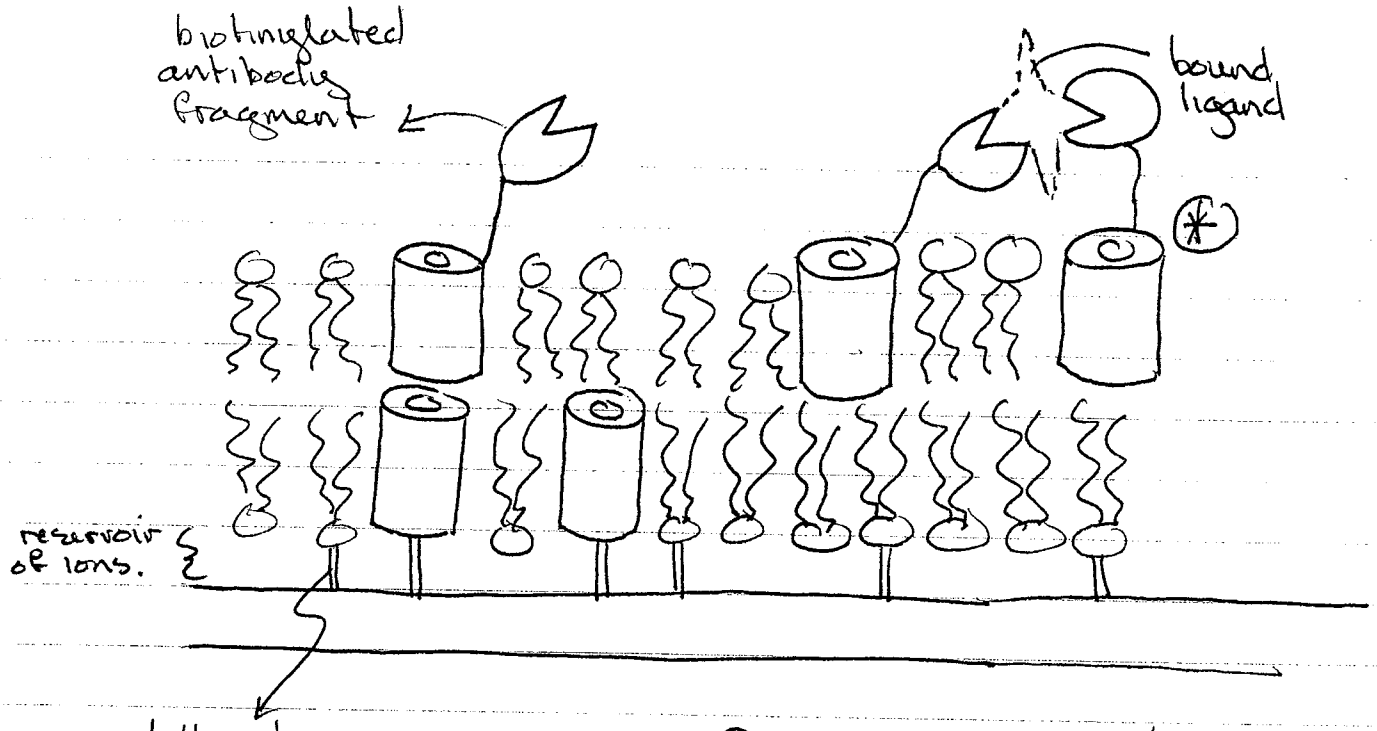

(*) ligand-bound & clustered gramicidin no longer available to conduct ions.

The antibody can be specific to a certain ligand. The lipids are synthetic models of archaebacterial lipids to maximize long-term stability.
Tethered gramicidin in the lower monolayer only conducts ions when gramicidin in the upper layer is free to diffuse. When bound to ligand, ion conductance declines.

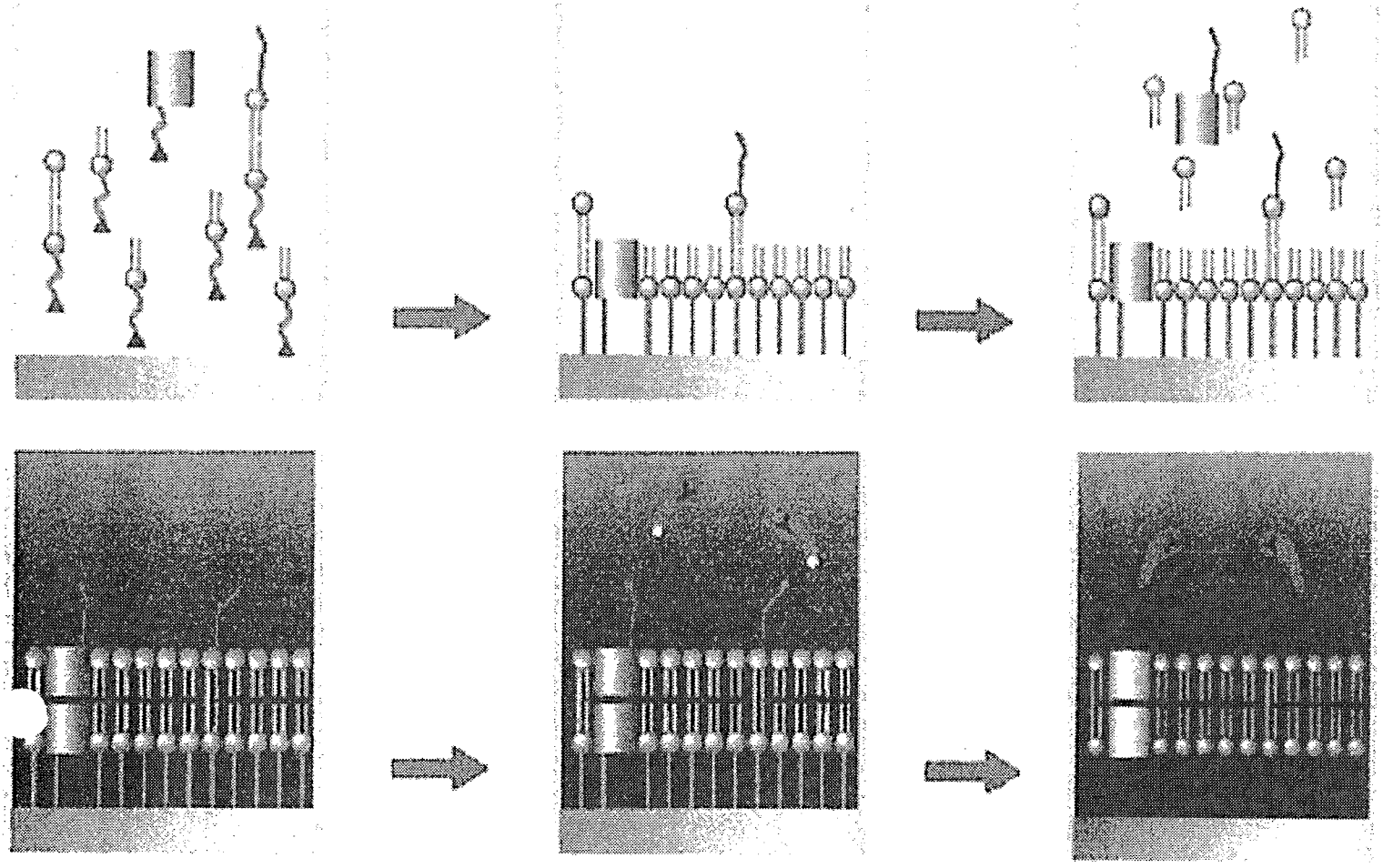

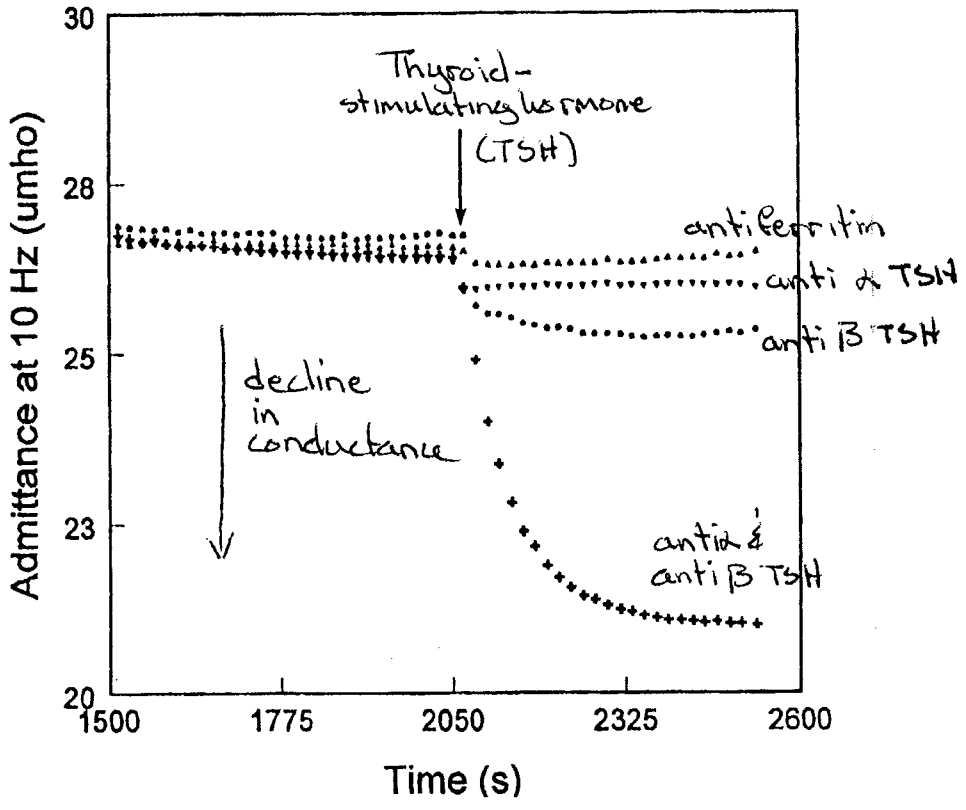

anti-ferritin gramicidin.

& normalized rate of decline in admittance.

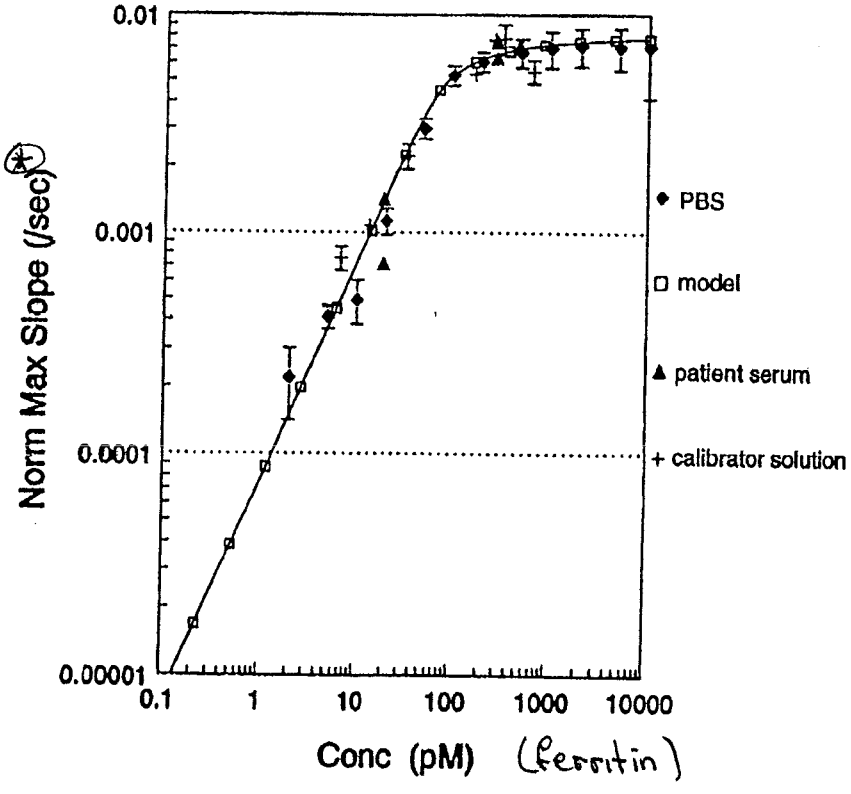

source: Cornell et al. 1999

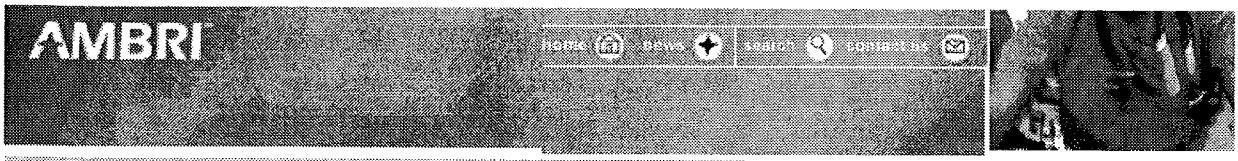

technology

Ambri's core technology, the Ion Channel Switch (ICS™), consolidates more than a decade of research by the Australian Membrane and Biotechnology Research Institute (AMBRI), CSIRO and the University of Sydney.

The ICS™ technology is a novel biosensor technology based upon a synthetic self assembling membrane. The membrane acts like a biological switch and is capable of detecting the presence of specific molecules, and signalling their presence by triggering an electrical current.

Many competing biosensor technologies rely on colormetric changes of solutions, measured photometrically for a quantitative reading. Ambri's ICS™ biosensor has the ability to detect a change in ion flow upon binding with the target molecule resulting in a rapid result currently unachievable using existing technologies.

The Ambri ICS™ biosensor may have applications in various markets including healthcare, food, environmental and other areas.

Click to learn more about the Ambri ICS™ technology.

A once in a decade breakthrough
...Precisely

66

nature

nature 05 June 1997

letters to nature

Nature **387**, 580 - 583 (1997); doi:10.1038/42432

A biosensor that uses ion-channel switches

B. A. CORNELL[1], V. L. B. BRAACH-MAKSVYTIS[1], L. G. KING[1], P. D. J. OSMAN[1], B. RAGUSE[1], L. WIECZOREK[1] & R. J. PACE*

[1] Co-operative Research Centre for Molecular Engineering & Technology, 126 Greville Street, Chatswood NSW 2067 Australia
* Chemistry Department, Faculty of Science, Australian National University, Canberra, ACT, Australia.

Correspondence and requests for materials should be addressed to B.A.C. (e-mail: bcornell@ambri.com.au).

Biosensors are molecular sensors that combine a biological recognition mechanism with a physical transduction technique. They provide a new class of inexpensive, portable instrument that permit sophisticated analytical measurements to be undertaken rapidly at decentralized locations. However, the adoption of biosensors for practical applications other than the measurement of blood glucose is currently limited by the expense, insensitivity and inflexibility of the available transduction methods. Here we describe the development of a biosensing technique in which the conductance of a population of molecular ion channels is switched by the recognition event. The approach mimics biological sensory functions and can be used with most types of receptor, including antibodies and nucleotides. The technique is very flexible and even in its simplest form it is sensitive to picomolar concentrations of proteins. The sensor is essentially an impedance element whose dimensions can readily be reduced to become an integral component of a microelectronic circuit. It may be used in a wide range of applications and in complex media, including blood. These uses might include cell typing, the detection of large proteins, viruses, antibodies, DNA, electrolytes, drugs, pesticides and other low-molecular-weight compounds.

Molecular Switching in Biosensors

Auburn University

< Back to Projects List

Summary

A biosensor is a device that incorporates a biological sensing element in close proximity to or integrated with a physical signal transducer. The sensing elements accomplish recognition from the binding, which occurs between biorecognition molecules and target analytes. Transduction is the physicochemical perturbation caused by this binding, which enables recognition of the triggered change by some device.

To detect a small number of binding events, a single binding event must be amplified. Here, we put forward a molecular switch capable of converting a single binding event into the movement of about one million ions per second. In this switch, a single binding, amplified by the release of the stored free electrochemical energy, leads to a dynamic signal that is large compared to the noise in the measuring system.

This approach is adapted from biological receptors, which convert chemical signals into currents in ion channels. The molecular switches in this work are artificial ion channels constructed by modular design from molecular pores and gates. The currents through these channels can be registered by conventional methods. The molecular switches can be triggered by various sensing elements such as antibodies, antibody fragments, polypeptides, DNA, RNA, and ion sensitive molecules. The small size and planar architecture of the molecular switches allow them to become components of a microelectronic circuit. The switches can be used for detection of proteins, toxins, viruses, bacteria, and ions. The ion channel assembled from molecules of Amphotericin B and Cholesterol are immobilized in bilayers and in monolayers on the liquid/gas and liquid/solid interfaces. Bilayers are formed from the spreading suspensions of phospholipid vesicles containing Amphotericin B and Cholesterol molecules. Studies of surface pressure-surface area isotherms of the monolayers show that Amphotericin B and Cholesterol form a complex with a 2:1 stoichiometry. These complexes aggregate by 2, 3, etc., and form ion channels in bilayers and multilayers transferred on solid substrates. The ion channels in bilayers are fast with millisecond dwell times and amplitudes in a range of 4-400 pS.

Features of the Molecular Switch
- High sensitivity from 1 to 100 binding events
- Gain 1´106
- Rapid, ~1 ms
- Modular molecular design
- Can be triggered by a large variety of sensing elements
- Reversible
- Electrical output signal
- Small size and planar architecture
- Consumes no external energy

A tetraethylammonium blocker controls the ion channels. The ion channels are reconstituted on the surface of 7nm mesopore silicon wafer made by Sandia National Laboratories. A laser ion-channel reader is designed and a principle proved. These ion channels can be used as fast and sensitive molecular switches in biosensors.

Click images to enlarge:

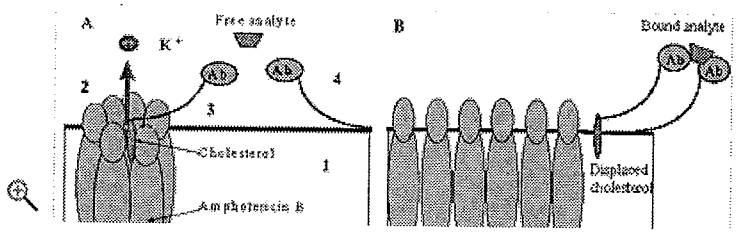

68